AGU PUBLICATIONS

Global Biogeochemical Cycles

RESEARCH ARTICLE
10.1002/2016GB005548

Key Points:
- Carbon dynamics were simulated through improved model parameterization
- Fire disturbance caused large direct carbon emission in North America
- The contribution of fire to net ecosystem carbon flux was small during recent decades

Correspondence to:
G. Chen,
auburncgs@gmail.com

Citation:
Chen, G., D. J. Hayes, and A. David McGuire (2017), Contributions of wildland fire to terrestrial ecosystem carbon dynamics in North America from 1990 to 2012, *Global Biogeochem. Cycles*, *31*, 878–900, doi:10.1002/2016GB005548.

Received 9 OCT 2016
Accepted 2 MAY 2017
Accepted article online 5 MAY 2017
Published online 27 MAY 2017

Contributions of wildland fire to terrestrial ecosystem carbon dynamics in North America from 1990 to 2012

Guangsheng Chen[1], Daniel J. Hayes[2], and A. David McGuire[3]

[1]Environmental Sciences Division, Oak Ridge National Laboratory, Oak Ridge, Tennessee, USA, [2]School of Forest Resources, University of Maine, Orono, Maine, USA, [3]Alaska Cooperative Fish and Wildlife Research Unit, U.S. Geological Survey, University of Alaska Fairbanks, Fairbanks, Alaska, USA

Abstract Burn area and the frequency of extreme fire events have been increasing during recent decades in North America, and this trend is expected to continue over the 21st century. While many aspects of the North American carbon budget have been intensively studied, the net contribution of fire disturbance to the overall net carbon flux at the continental scale remains uncertain. Based on national scale, spatially explicit and long-term fire data, along with the improved model parameterization in a process-based ecosystem model, we simulated the impact of fire disturbance on both direct carbon emissions and net terrestrial ecosystem carbon balance in North America. Fire-caused direct carbon emissions were 106.55 ± 15.98 Tg C/yr during 1990–2012; however, the net ecosystem carbon balance associated with fire was −26.09 ± 5.22 Tg C/yr, indicating that most of the emitted carbon was resequestered by the terrestrial ecosystem. Direct carbon emissions showed an increase in Alaska and Canada during 1990–2012 as compared to prior periods due to more extreme fire events, resulting in a large carbon source from these two regions. Among biomes, the largest carbon source was found to be from the boreal forest, primarily due to large reductions in soil organic matter during, and with slower recovery after, fire events. The interactions between fire and environmental factors reduced the fire-caused ecosystem carbon source. Fire disturbance only caused a weak carbon source as compared to the best estimate terrestrial carbon sink in North America owing to the long-term legacy effects of historical burn area coupled with fast ecosystem recovery during 1990–2012.

1. Introduction

Fire disturbance could significantly affect terrestrial ecosystem carbon dynamics in multiple ways, with the net effect determined by integrating both short-term and long-term effects on carbon pools and fluxes. In the short term, fire effects on carbon storage are determined by direct carbon emissions from combustion, vegetation and organic matter recovery rates, and legacy effects from prior fires [*Kurz et al.*, 2008a; *Kashian et al.*, 2006; *Hurteau and Brooks*, 2011]. Fire can cause large direct carbon emissions by consuming surface fuels including living and standing dead biomass, coarse woody debris (CWD), aboveground fine litter, and near-surface soil organic matter (SOM) [*Meigs et al.*, 2009]. The combustion of these organic matter pools during fire releases greenhouse gases, including carbon dioxide (CO_2), methane (CH_4), and nitrous oxide into the atmosphere, which can have consequences for atmospheric composition and radiative forcing. Global fire emissions are reported to be one of the major factors controlling interannual variability of atmospheric CO_2 and CH_4 [*Bousquet et al.*, 2006; *van der Werf et al.*, 2004]. Fire consumption may also result in large nutrient losses from organic matter pools and releases inorganic nutrients to the soil, potentially increasing post-fire vegetation growth in the short term [*Hurteau and Brooks*, 2011]. Fire influences ecosystem composition and structure by providing a competitive advantage in postfire environmental conditions for some species, which has implications for productivity and vegetation dynamics in succession after fire [*Johnson*, 1992]. Fire can also lead to increases in soil temperature and moisture in the soil surface, thus altering soil thermal and chemical dynamics in the short term [*Yi et al.*, 2009, 2010].

Over the long term, fire effects on terrestrial carbon stocks are a function of the balance between carbon losses from direct fire emissions and dead organic matter decomposition and carbon gains from vegetation regeneration and growth [*Kashian et al.*, 2006]. The portion of killed vegetation biomass that was not consumed by fire will influence the ecosystem soil and litter carbon and nutrient dynamics over the long term. The amount and decomposition rate of dead organic matter that remains following a fire event are

determined by the burn severity, the vegetation, and environmental conditions [*Meigs et al.*, 2009]. After fire, the recovering ecosystems will gradually transition from a carbon source to a carbon sink, and with sufficient time the ecosystems will absorb all of the carbon lost from both direct and indirect sources [*Kashian et al.*, 2006]. Overall, the net carbon balance will be close to zero over the fire cycle and the length of which is determined by environmental factors (e.g., climate), ecosystem properties (e.g., soil properties, vegetation type, and fuel load), and fire characteristics (e.g., fire intensity, severity, and combustion completeness) [*Hurteau and Brooks*, 2011]. For example, studies have shown that fire results in permafrost thaw from a reduction in soil organic layer depth that recovers on the scale of decades to centuries in the boreal forests of North America [*Genet et al.*, 2013; *Yuan et al.*, 2012; *Kasischke and Hoy*, 2012], illustrating the long-term legacy effects of fire on permafrost and carbon cycling in arctic and boreal ecosystems.

Fire suppression activities such as prescribed fire and litter raking have been thought to effectively reduce wildland fire frequency and intensity in North America during the recent century [*Hurtt et al.*, 2002]; however, due to climate warming and intensifying drought conditions, fire intensity and frequency were still found to increase during recent decades and are predicted to increase in the future [*Flannigan and van Wagner*, 1991; *Harden et al.*, 2000; *Kasischke and Turetsky*, 2006; *Balshi et al.*, 2009; *Yue et al.*, 2013]. The fire record in the U.S. indicates that burn area and severity have significantly increased from the early 1980s to the present [*Yang et al.*, 2015a]. The largest burn area years on record have occurred during the most recent two decades in Alaska (2004, 2005, and 2015) and California (2004, 2006 and 2015). *Yue et al.* [2013] indicated that the length of the wildfire season in the western U.S. has increased by roughly two and a half months since the mid-1980s, mostly due to earlier snowmelt, and they also predict a 20–50% increase in burn area from present to 2050. Additionally, *Balshi et al.* [2009] predict a 3–6 times increase in annual burn area for boreal North America over the 21st century based on two future climate change scenarios.

Many studies have been conducted over the past two decades to estimate fire behavior and ecological impacts in North America based on remote sensing [e.g., *Wiedinmyer and Neff*, 2007], field observations [*French et al.*, 2011; *Kasischke and Hoy*, 2012; *de Groot et al.*, 2009], and modeling simulation [e.g., *Balshi et al.*, 2007, 2009; *Zhuang et al.*, 2002; *Yue et al.*, 2013; *Yang et al.*, 2015a, 2015b]. To date, these studies have focused on (a) fire-caused direct carbon emissions rather than net ecosystem carbon budget, (b) smaller subregions of North America rather than the continental scale, (c) use of book-keeping approaches with fixed parameter assignments for C budget assessment, and/or (d) short-term analyses instead of making use of the full time periods of available fire records. As compared to postfire carbon dynamics, it is more difficult to quantify the fire-caused net ecosystem carbon balance due to the long-term legacy effects from historical fires, which can significantly influence the estimation accuracy of fire-caused net carbon balance in contemporary study periods [*Kelly et al.*, 2016]. As such, there lacks a comprehensive, consistent, and long-term estimate for the effects of fire disturbance on the continental-scale terrestrial carbon budget in North America [*Kasischke et al.*, 2011]. With improved technology in remote sensing monitoring, increasing investment in regional field data collection and improved understanding of mechanisms, it is now possible to integrate large-scale fire data sets with mechanistic models. Therefore, in this study, we integrate information that relates fire effects to various environmental conditions and ecosystem characteristics with improvements in the fire-related parameterization of an ecosystem process model. Several studies [e.g., *Hayes et al.*, 2012; *King et al.*, 2012] estimated a large carbon sink during 1990s and 2000s in North America based on multiple approaches, but there is no consensus on the contributions of wildland fire from these studies [*King et al.*, 2015]. The objective for this study is to provide a more comprehensive and consistent estimation of fire-caused direct carbon emissions and net ecosystem carbon balance based on available burn area data across North America.

2. Methods

2.1. General Model Description

In this study, the impacts of fire disturbance on carbon dynamics were simulated with an updated version of the Terrestrial Ecosystem Model (TEM version 6.1), modified for this study to improve the representation of carbon pool transfers resulting from fire and other disturbances. TEM has been well documented and used to examine terrestrial carbon dynamics under changing environmental factors (including climate, atmospheric CO_2, nitrogen deposition, land use change, disturbance, and ozone pollution) at various spatial

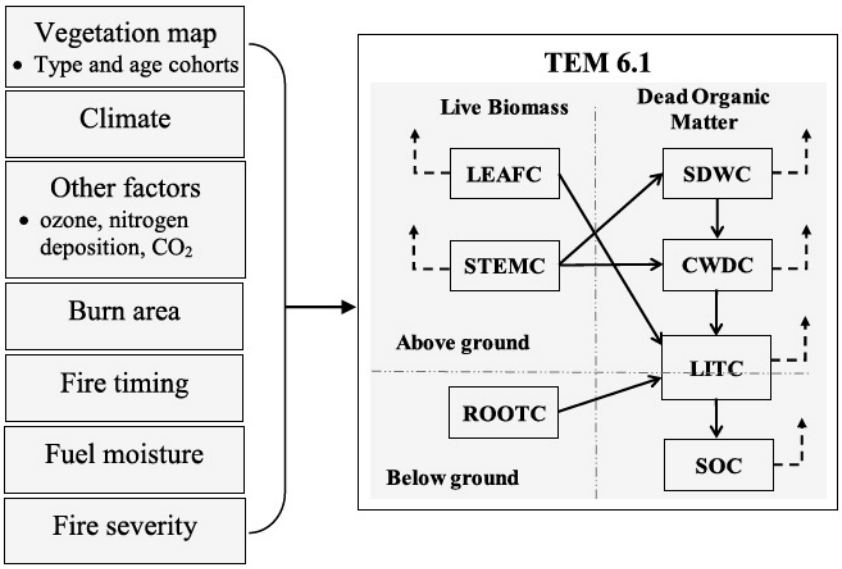

Figure 1. The brief structure for fire submodel in the TEM6.1. Note: SDWC: standing dead wood carbon pool, CWDC: coarse woody debris carbon pool, SOC: soil organic carbon, LITC: litter carbon pool. The solid arrows represent the dead biomass allocation directions; the dashed arrows represent the direct carbon emission from each fuel component.

scales [*McGuire et al.*, 2000a; *Balshi et al.*, 2007]. Model estimates of carbon fluxes and stocks have been extensively evaluated in many previous studies at site and regional scales [e.g., *McGuire et al.*, 2000b; *Zhuang et al.*, 2002, 2003; *Amthor et al.*, 2001; *Balshi et al.*, 2007, 2009; *Lu et al.*, 2015; *Kelly et al.*, 2016]. TEM has been used to estimate fire disturbance effects on ecosystem carbon fluxes and storage, showing good performance as evaluated against field observational data in boreal North America [*Bashi et al.*, 2007; *Zhuang et al.*, 2003] and compared to multiple constraints at the pan-boreal scale [*Hayes et al.*, 2011]. In this study, we modified TEM version 6.0 [*Hayes et al.*, 2011] by adopting two modules from two other versions of TEM: the TEM-Dynamic Vegetation Model [*Euskirchen et al.*, 2009; *Yuan et al.*, 2012] and TEM-Hydro [*Felzer et al.*, 2009]. The major modifications include (1) separating the live biomass pool into different plant components (i.e., leaf, coarse root, fine root, and stem pools); (2) partitioning the dead organic matter pool into four pools: aboveground fine litter, coarse woody debris (CWD), belowground litter, and soil organic carbon (SOC); and (3) adding a standing deadwood (SDW) carbon pool, which is used to resolve in more detail important ecological dynamics driven by fire and other disturbances. The performance of the model updates was evaluated in this study against field data and other studies (see section 4).

In TEM, the net ecosystem carbon balance (NECB) is estimated as [*McGuire et al.*, 2000a]

$$\mathrm{NECB} = \mathrm{GPP} - Ra - Rh - Ec - Ep - Ed - El \tag{1}$$

where GPP is the gross primary productivity, *Ra* is plant autotrophic respiration, *Rh* is heterotrophic respiration, *Ec* is carbon emission during the conversion of natural ecosystems to agriculture, *Ep* is the sum of carbon emission from the decomposition of agricultural and wood product, *Ed* is direct carbon emission from disturbance, and *El* is carbon leaching from terrestrial ecosystem to aquatic system. NECB represents the change in total carbon storage across all pools, or the sum of all carbon fluxes into (sink, with positive values) and out of (source, with negative values) the ecosystem over a given time step [*Chapin et al.*, 2006].

In TEM6.1, a fire module was specifically developed to track fire effects on terrestrial carbon and nitrogen dynamics (Figure 1). Within this framework, the TEM cohort module was used in this study to select the burned vegetation cohorts and to track the identity, area coverage, and age (time since last disturbance) of vegetation cohorts within each grid cell. The principles and procedure of the subgrid cohort module are described in more detail by *Hayes et al.* [2011], and its implementation for this study is described below. The fire characteristics data, such as burn area and fire timing, are incorporated with fuel characteristics (e.g., fuel loads, fuel components, and fuel moisture), initial vegetation map, and climate conditions (e.g.,

precipitation and air temperature) to generate the model parameters including fire-caused mortality and fuel combustion completeness for different fuel components.

TEM simulates eight components of fuels including live leaf, stem, and root fuel components; SDW (standing dead stems and branches, for woody plants only); CWD (diameter $>$ 5 mm; including fallen dead stems and most dead branches, for woody plants only); aboveground fine litter (diameter $\leq$ 5 mm, including dead leaves, fine branches, and barks); belowground litter (i.e., dead roots); and SOM (the duff and mineral soil layer) (Figure 1). The forest floor fuel components include aboveground fine litter and top-layer partially decomposed organic material (also known as duff, is composed of soil organic matter (SOM), partially decomposed aboveground and belowground litter [*French et al.*, 2004]). The duff is also defined as the fermentation and humus layer of the soil located between the A horizon (or uppermost soil mineral horizon) and the litter layer, which is an important fuel component in the boreal region. In the analysis, we also combined the belowground and aboveground litter as total litter pool (LIT). The dynamics of these fuel components were simulated by the modified TEM6.1 in terms of burn severity of overstory live biomass (i.e., leaf, root, and stem carbon transfers) and combustion completeness of surface and belowground organic matter (i.e., litter and SOM). The carbon transfers among the live biomass and dead organic matter pools and to the atmosphere are illustrated in Figure 1.

In TEM6.1, monthly direct carbon emissions (total fuel consumption (TFC)) from fire were estimated as

$$\mathrm{TFC} = \mathrm{BFC} + \mathrm{FFC} + \mathrm{DWDFC} \tag{2}$$

where BFC is the live biomass (i.e., live leaf, stem, and root) fuel consumption, FFC is the forest floor fuel consumption, and DWDFC is the dead woody debris fuel consumption, which includes the SDW and CWD pools. The estimation of direct carbon emissions from each of these fuel components and their related parameterizations is described below.

2.2. Model Input Data and Parameterization Methods

2.2.1. Burn Area Data

The annual burn area data used in this study were obtained from multiple sources, including field observation data, remote sensing of fire perimeters, and model simulations (Table 1). For Alaska, we obtained burn area data from the Bureau of Land Management Alaska Fire Service (BLM AFS), covering the period of 1940–2012 [http://afs.ak.blm.gov/; *Kasischke et al.*, 2002]. For Canada, we obtained the polygon burn area perimeter data from the Canadian National Fire Database (CNFDB; http://cwfis.cfs.nrcan.gc.ca/ha/nfdb). The CNFDB data generally cover the period from 1920 to 2012, though for most provinces, the full records start in the 1980s [see *Kurz et al.*, 2008b; *Stinson et al.*, 2011]. Only a few provinces have records starting at 1920. Burn area data for those provinces that are not available before the 1980s were reconstructed based on the calculated fire return interval (FRI) and vegetation cohort age according to the approaches described in *Balshi et al.* [2007]. This fire data set only includes large fires (burn area $>$ 200 ha [*Kasischke et al.*, 2011]) events, but it accounts for the majority of the burned area that occurs across Canada's boreal forest region (http://cwfis.cfs.nrcan.gc.ca/ha/nfdb). For the conterminous United States (CONUS), we obtained the polygon fire records from the U.S. Monitoring Trends in Burn Severity (MTBS) for the period of 1984–2012 (http://www.mtbs.gov/). For Mexico, there were no available fire records, so we used the gridded (0.25° spatial resolution), monthly burn area data from the Global Fire Emission Database Version 4 (GFED4) [*Giglio et al.*, 2013], which covers the period of 1996 to present.

We compiled and gridded the data from the various fire records by decomposing each burn polygon into 1 km × 1 km pixels labeled as "burned" (with pixels outside of the polygons labeled "unburned"). Then we upscaled from 1 km × 1 km to 0.25° × 0.25° spatial resolution with a sum aggregation method in ArcGIS 10.3.1. In this way, the number of burned 1 km pixels in each 0.25° grid cell was counted in each year. The most commonly used method for reconstructing historical fire regimes is fire frequency [*Schmoldt et al.*, 1999]. Based on the gridded burn area data, we calculated the mean FRI for each grid cell as the ratio of total cell area to mean annual burn area [*Johnson*, 1992; *Barrett et al.*, 2010]. We used the FRI and stand age information to reconstruct fire history and vegetation cohort dynamics for the periods without burn area records during 1000–2012 for model equilibrium, spin-up, and transient runs (see methods described below).

Table 1. Burn Area Data Sources and Characteristics

Regions	Data Source	Inventory Fire Data Periods	FRI-Based Periods	Affected/Total Grid Cells	Mean Burn Area (km^2/yr)
Alaska	BLM AFS	1940–2012	1000–1939	1,579/4,383	3,246
Canada	CNFDB	1920–2012	1000[a]	8,154/25,653	17,627
CONUS	MTBS	1984–2012	1000–1983	4,795/13,049	16,331
Mexico	GFED4	1996–2012	1000–1995	1,741/2,714	11,068

[a]Fire records start at different time periods for various provinces in Canada [see *Kurz et al.*, 2009] and CONUS: The 48 conterminous U.S. states.

2.2.2. Burned Vegetation Types and Area

The burned cohorts and vegetation types are determined primarily based on the 1 km spatial resolution North American Land Change Monitoring System 2005 (http://landcover.usgs.gov/nalcms.php) data set produced by the Commission for Environmental Cooperation. The NLCD2001 land cover data (http://www.mrlc.gov/nlcd01_data.php) was used as an auxiliary data to develop a better land cover map for Alaska. The International Geosphere-Biosphere Programme DISCover global land cover data [*Loveland et al.*, 2000] and global potential vegetation map [*Ramankutty and Foley*, 1999] were also used to assist in generating potential vegetation map (i.e., replacing managed land cover including pasture, cropland, and urban with natural vegetation). The boreal boundary map from *Brandt* [2009] was used to depict the boreal forest types in Canada and Alaska. These vegetation-type categories were regrouped into the corresponding plant functional types used by TEM6.1 (see Figure 2). For the years with available burn area polygon data in Alaska (1940–2012), Canada (1920–2012), and CONUS (1984–2012), the annual burn polygons were overlaid with the land cover data to obtain the burned area for each vegetation type at 1 km spatial resolution. The total burned area of each vegetation type within a 0.25° grid cell was then aggregated by summing up burned area for all 1 km grid cells in ArcGIS 10.2. For Mexico, the 0.25° burn area data from GFED4.0 were directly used to overlay with the 0.25° land cover map to obtain the burned vegetation types and area in each grid cell. To generate the burned vegetation cohort and area for those years without burn area data (before 1940 for Alaska, before 1920 for Canada, before 1984 for CONUS, and before 1996 for Mexico), we used the generated mean FRI data and stand age (i.e., the years since the previous disturbance event) to determine the burned vegetation types and area. When the stand age of a vegetation cohort equals to the mean FRI of its grid cell, the cohort is burned. We used the approach described by *Hayes et al.* [2011] to track the dynamics of vegetation and age cohorts in each grid cell. When a

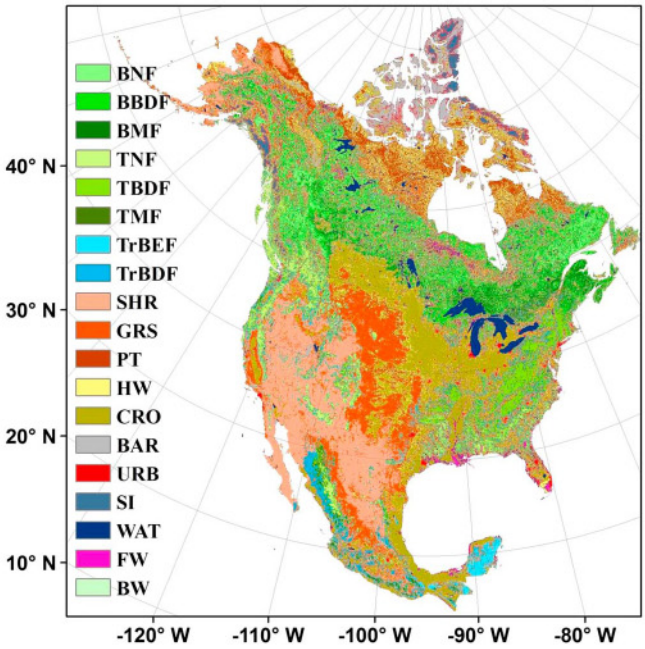

Figure 2. Distributions of major vegetation types at 1 km × 1 km spatial resolution in North America during 2000s. BNF: boreal needleleaf forest, BBDF: boreal broadleaf deciduous forest, BMF: boreal mixed forest, TNF: temperate needleleaf forest, TBDF: temperate broadleaf deciduous forest, TMF: temperate mixed forest, TrBEF: tropical/subtropical broadleaf evergreen forest, TrBDF: tropical/subtropical broadleaf deciduous forest, SHR: shrubland, GRS: grassland, PT: polar tundra, HW: herbaceous wetland, CRO: cropland, BAR: barren land, URB: urban/built-up land, SI: snow and ice, WAT: water, FW: forested wetland, BW: boreal woodland (grassland with sparse trees).

Table 2. Allocation for Unconsumed Dead Biomass After Fire

Fuel Components	SDW	Litter	CWD
Leaf	–	1.0	–
Stem	0.6[a]	0.2[a]	0.2[a]
Root	–	1.0	–
SDW	–	–	1.0

[a]Slightly varied for different ecoregions in Canada according to the observational data [*Kurz et al.*, 2008a].

cohort in a grid cell is burned, a child cohort is produced. The old cohort (i.e., the parent cohort) is maintained with the remaining living biomass and the same environmental conditions, while the new cohort (i.e., the child cohort) regrows from stand age 0 but otherwise inherits the ecosystem type and other environmental conditions—including soil physical and chemical properties and climate condition—from its parent cohort [*Balshi et al.*, 2007]. To avoid too many cohorts within a grid cell, the cohorts with stand age higher than a threshold age will be combined as one. The threshold age is determined if the differences in carbon, nitrogen, and water exchange rates among cohorts are within a certain tolerance level (i.e., 0.5 g C/m^2, 0.1 g N/m^2, and 0.2 mm for carbon, nitrogen, and water, respectively) during 10 consecutive years. While this approach realistically simulates the effects of stand age on microenvironment, carbon, and nitrogen dynamics, it does not however simulate species composition dynamics associated with postfire ecosystem succession (e.g., there is no shrub or grass stage in postfire black spruce stands in this approach).

2.2.3. Fire Timing

Previous studies [e.g., *Turetsky et al.*, 2011; *Genet et al.*, 2013] have indicated that fuel loads, fire severity (represented by vegetation mortality in this study [*Rogers et al.*, 2015]), and combustion completeness (CC) are significantly influenced by the month of fire occurrence; therefore, it is important to include the fire timing information to simulate fire-caused carbon dynamics. The burn area records for Alaska, Canada, and CONUS have provided fire month data for fire events. Based on the monthly fire polygon data, we averaged across all fire months within 1 year to get the average fire month for each grid cell at 1 km spatial resolution. The 1 km fire month data were then aggregated to 0.25° resolution data using the majority method (i.e., to identify the month with the highest burned area during the recorded fire periods) in ArcGIS. For some fire records without fire timing information, we used the average fire months from GFED4 data as a replacement. For Mexico, the monthly 0.25° GFED4 fire month data were used. We chose the month with the highest burn area within 1 year as the fire month from GFED4.

2.2.4. Fire-Caused Mortality and Biomass Consumption

Fire-caused live biomass mortality is influenced by the timing, intensity, and frequency of fire, along with ecosystem biotic and abiotic properties. In boreal North America, most fires occur as stand-replacing crown fires [*Stocks and Kauffman*, 1997]. According to *Balshi et al.* [2007] and *Kurz et al.* [2008b], fires in boreal forests generally cause over 95% (varied slightly for different provinces in Canada) vegetation mortality, which is higher than the 80% average tree mortality estimated by a recent study [*Rogers et al.*, 2015]. For CONUS, we aggregated the 30 m LANDFIRE fire severity categories to 0.25° spatial resolution. The LANDFIRE model (http://www.landfire.gov/fireregime.php) produced five fire regime condition classes (FRCC) for U.S. forest regions based on the fire return interval and average aboveground biomass mortality for fire events: low/mixed (0–35 years; 40% mortality), replacement (0–35 years; 75% mortality), low/mixed (35–200 years; 40% mortality), replacement (35–200 years; 75% mortality), and replacement (200+ years; 75% mortality) severity. The maximum mortality for aboveground biomass of shrub and herbaceous plants was set to 100% according to *van der Werf et al.* [2010] and *Ito and Penner* [2004], while mortality for roots was set to 30%.

The killed biomass is partly consumed by fire, while the remaining is partitioned among the SDW, CWD, and aboveground and belowground litter pools (Table 2). The portion of direct consumption of live biomass is determined by the vegetation mortality and CC parameters. The CC parameter values for killed trees for Alaska and Canada were obtained from the literature [*Balshi et al.*, 2007; *Kurz et al.*, 2008a, 2008b; *Stinson et al.*, 2011], while we applied the CC parameters used by GFED4 [*Giglio et al.*, 2013] for CONUS and Mexico. The CC for tree root biomass was assumed to be 0. The CC values for aboveground biomass of shrub and herbaceous plants were set at 80% according to *van der Werf et al.* [2010]. The CC for roots of shrub and herbaceous plants was set as 10%.

Table 3. Consumption Completeness (CC) and Estimation Methods for Different Woody Fuel Components

Fuel Components	CC Range	Actual CC	Literature Reference(s)
Leaves	0.8–1.0		*van der Werf et al.* [2010]
Stems	0.2–0.4[a]		*Balshi et al.* [2007]; *Kurz et al.* [2008a, 2008b]; LANDFIRE FRCC
Aboveground fine litter	0.4–1.0	Equation (4)	*Turetsky et al.* [2011]; *de Groot et al.* [2009]
CWD		Equation (5)	*Kasischke and Hoy* [2012]
SOM (duff)	<15 cm topsoil layer	Equation (4)	*Turetsky et al.* [2011]; *de Groot et al.* [2009]
SDW		Equation (5)	*Kasischke and Hoy* [2012]

[a]For Alaska and Canada, the consumption completeness of stem wood parameters is obtained from *Balshi et al.* [2007] and *Kurz et al.* [2008a, 2008b]; for CONUS, the consumption fractions are scaled based on the LANDFIRE FRCC data; for Mexico, the GFED4 combustion completeness parameters are used.

The parameters of CC for different regions are shown in Table 3. The biomass fuel consumption (BFC) was then calculated as

$$BFC = \sum_{i=0}^{3} BA \times FL_i \times FM_i \times CC_i \quad (3)$$

where BA is the burn area (m^2), FL is the fuel load (g biomass/m^2), FM is fuel mortality (%), and i represents the live biomass components (1: leaf, 2: stem, 3: root).

2.2.5. Calculations of Dead Organic Matter Consumption

The consumption of dead organic matter including aboveground fine litter, belowground litter, SDW, and CWD is determined by many factors including fire intensity, topography, climate conditions, and fuel loads. The best fit equation from *de Groot et al.* [2009] was applied to calculate FFC for the boreal forest region of North America. This equation relates the FFC to the monthly drought code (DC_m) and fuel loads.

$$\ln(FFC) = a + b1 \times \ln(FFL) + b2 \times \ln(DC_m) \quad (4)$$

where $a = -4.252$, $b1 = 0.671$, and $b2 = 0.71$ according to *de Groot et al.* [2009]; FFC is the forest floor fuel consumption (kg biomass/m^2); FFL is the forest floor fuel load (kg biomass/m^2) composed of aboveground fine litter (leaf litter, barks, and stem/branch litter with diameter ≤ 5 mm; CWD was not included) and duff layer; ln is the natural based log function; and DC_m is the monthly drought code.

The DC_m was computed using monthly air temperature, precipitation, and previous month DC_m data according to the method described in *Girardin and Wotton* [2009]. DC_m effectively represents fuel moisture condition and thus has been widely applied to estimate the effects of fuel moisture on combustion completeness [*de Groot et al.*, 2009; *Kasischke and Hoy*, 2012]. The mean DC_m during 1979–2010 for North America is shown in Figure 3. Higher fuel drought degree values were found in central Alaska, northeastern and central Canada, western CONUS, and northern Mexico. The fuel consumption rate increases with DC_m (Figure 3).

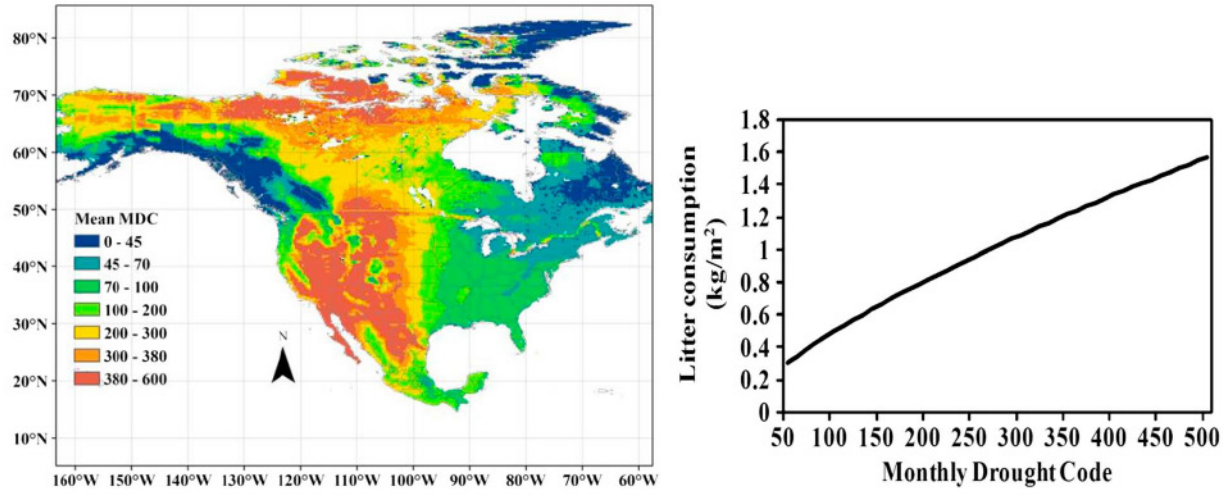

Figure 3. Spatial distribution of mean monthly drought code (DC_m) in North America during 1979–2010 (left) and sensitivity of forest floor fuel consumption with varied DC_m. Note that higher DC_m indicates drier forest floor fuel loads (including ground litter and soil duff).

Table 4. Model Experiment Designs

Experiment Name	Environmental Factors[a]	Actual Burn Area	FRI-Based Burn Area
ALL_FIRE (experiment 1)	1900–2012	P1–2012[b]	1000–P1
ALL_NOFIRE (experiment 2)	1900–2012	–	–
FIRE_ONLY (experiment 3)	1000[c]	P1–2012	1000–P1
ALL_FRI (experiment 4)	1900–2012	–	1000–2012
BASELINE1 (experiment 5)	1900–2012	–	1000–P1
BASELINE2 (experiment 6)	1900–2012	P1–1990	1000–P1

[a]Environmental factors include climate, atmospheric CO_2, ozone, and land use and land cover.
[b]P1 represents varied start periods for different regions (Alaska: 1940, Canada: 1920, CONUS: 1984, Mexico: 1996); FRI-based burn area and cohort is used prior to available actual burn area data.
[c]Mean climate data from 1979 to 1988 are used, while the earliest data are used for other factors.

Since TEM6.1 does not directly simulate carbon distribution with soil depth, we used the carbon stock-depth relationship equations from *Turetsky et al.* [2011] to calculate topsoil organic layer (duff) depth for different landscape classes. Due to coarse spatial resolution (0.25°), we only separated landscapes into two categories: flat lowland and flat upland; therefore, the power law equations for these two types were used in this study. The maximum burn duff depth can be 25 cm in the boreal North America according to *Turetsky et al.* [2011] and varied with vegetation composition [*Rogers et al.*, 2015], but ultimately, we set the maximum burn duff depth to 15 cm according to *van der Werf et al.* [2010], which is the average burn depth under the influences of middle fire size as inferred from *Turetsky et al.* [2011]. The actual burn depth of duff was then scaled with DC_m (equation (4)).

The dead woody debris fuel consumption (DWDFC; kg/m^2) was estimated using the equation from *Kasischke and Hoy* [2012].

$$\mathrm{DWDFC} = -0.131 + 0.108\,\mathrm{DWD1} + 0.436\,\mathrm{DWD2} + 0.00144\,\mathrm{DC}m \tag{5}$$

where DWD1 is the SDW and CWD with diameter $>$ 7 cm (kg/m^2) including stems and large branches and DWD2 is the SDW and CWD with diameter $<$ 7 cm.

2.2.6. Other Model Input Data

Two types (static and dynamic variables) of other model input data were used to drive the TEM. The static variables include soil texture (percent of sand, clay, and loam), soil drainage condition (wet or dry), soil topography information (elevation, slope, and aspect), and potential vegetation map (assumed vegetation types in 1700 with no human activities). The dynamic variables include annual atmospheric CO_2 concentration, land use data (i.e., cropland, urban, pasture, and deforestation proportion) in 2005, detrended monthly climate data (precipitation, air temperature, and short-wave radiation), monthly tropospheric ozone level, and annual nitrogen deposition data. The spatial resolution of all data was 0.25° × 0.25° by latitude and longitude. The data source and generation methods for static data and for monthly climate data, land use data, and nitrogen deposition are described in *Wei et al.* [2014]. The monthly tropospheric ozone concentration data (AOT40 ozone exposure index: the accumulated hourly ozone concentration over a threshold of 40 ppb/h) was obtained from *Felzer et al.* [2005].

2.3. Model Simulations

2.3.1. Model Equilibrium and Spin-Up Runs

We used the mean climate data (average over 1979–2010), potential vegetation cohorts (year 1700), and earliest atmospheric CO_2 data (year 1860) and nitrogen deposition data (year 1860) to run the model and represent the model equilibrium status (initial condition) in year 1000. After the equilibrium run, a 900 year spin-up run was conducted (spin-up run ends at 1900). The mean climate data (averaged over 1979–1998) and the vegetation cohort data generated based on FRI-based fire history were used during the spin-up simulation, while all other input data were kept the same as in the equilibrium run.

2.3.2. Model Simulation Experiments

The fire-caused net ecosystem carbon balance is difficult to track due to the legacy effects and compounding effects from other environmental factors; therefore, six model simulation experiments were specifically designed to differentiate the effects of environmental factors, fire, and their interactions. The designs of the six experiments were shown in Table 4. Through these model experiments, we can derive

the fire effects (experiment 1 − experiment 2 − experiment 5 or experiment 1 − experiment 2 − experiment 6; including the interactive effects from environmental factors), environmental effects (experiment 1 − experiment 3; including interactive effects from fire), and effects of changing fire regime (experiment 1 − experiment 4) on ecosystem carbon dynamics during 1900–2012. Because of limitations associated with the available fire records, the analysis periods started from 1940, 1920, 1984, and 1996 for Alaska, Canada, CONUS, and Mexico, respectively. To summarize the direct carbon emission and NECB estimates for the entire North American land area, we used the data for the common time period of 1990–2012.

2.3.3. Model Evaluation

Although TEM has been extensively evaluated for its skill in simulating the effects of multiple environmental changes and disturbances on ecosystem processes, we reevaluated the performance using the modified version from this study (TEM6.1) in simulating carbon dynamics after fire disturbance. Simulation output was compared with field-based data at a series of fire chronosequence sites in Canada (Figure 4). The observational data for upland spruce forests were obtained from *Goulden et al.* [2011] and *Bond-Lamberty et al.* [2004]. The selected seven spruce forest stands were 1, 6, 15, 23, 40, 74, and 154 years old as of 2004. To conduct the model simulation, we selected a grid cell with >95% spruce forest and near the center of all seven sites. The actual climate and other environmental data for this grid cell were used to drive the model. The comparisons indicated that TEM model can effectively ($R^2 > 0.75$; $p < 0.01$) reproduce the interannual variation in GPP, net ecosystem production (NEP), and biomass following fire disturbance (Figures 4a–4c). However, TEM underestimated the forest floor carbon at the older (e.g., 74 and 154 years' old) spruce forest sites (Figure 4d). TEM also underestimated the CWD for the 23 and 40 years' old spruce forests (Figure 4e). This may be attributable to the lack of mechanisms in TEM for simulating the intrinsic (i.e., age-related) mortality of trees, which could cause increasing mortality with tree ages and remain constant after tree maturity. The TEM-simulated aboveground and belowground biomass was also compared with the observational data along the fire chronosequence gradient (i.e., stand ages 1, 4, 8, 14, and 28 years and mature forests) for a seasonal dry tropical forest in Mexico [*Vargas et al.*, 2008]. It indicated that TEM can better capture the aboveground biomass recovery (slope = 0.89 and $R^2 = 0.95$; Figure 5a) than that of the belowground biomass (slope = 0.52 and $R^2 = 0.70$; Figure 5b) following fire disturbance. Generally, TEM slightly overestimated both belowground- and aboveground biomass in the mature forests. In addition, the forest cohort age generated in this study was also compared with the inventory forest age data in Canada and CONUS [*Pan et al.*, 2012] (Figure 6). The results indicated that the spatial distribution of the generated age cohorts was generally consistent with the inventory data but tended to overestimate forest age, especially in southwestern Canada and southern US, indicating that our study may slightly overestimate direct carbon emissions. This might be because this study did not consider land use change or other nonfire disturbance events (such as insect outbreaks, forest harvesting, and storms/hurricanes).

2.4. Analysis Method and Model Uncertainty

Due to differences in available burn area data sets, the analysis periods for direct carbon emissions varied among Alaska (1940–2012), Canada (1920–2012), CONUS (1984–2012), and Mexico (1996–2012). We used 1990–2012 as the analysis period for analysis of carbon stocks and NECB since it represents the common (overlapping) period with available burn area data from all four regions. The FRI-based burn area from 1990 to 1995 was applied for Mexico since neither observed nor modeled burn area data are available for this period. Our purpose was to generate a comprehensive and consistent historical fire history in order to realistically represent the fire legacy effects before 1990.

Many factors will result in estimation uncertainty including burn area, mortality, combustion completeness, fuel load, emission factors, and other model input data and parameters. In this study, we only estimate the fire parameter uncertainties (i.e., vegetation mortality and combustion completeness). The uncertainties from input data and other model parameters were not explicitly analyzed here, considering that several previous studies have assessed these uncertainties [e.g., *French et al.*, 2004; *van der Werf et al.*, 2010]. We selected the burn severity parameters including live biomass, litter, and deadwood (including CWD) combustion completeness and vegetation mortality to conduct an uncertainty analysis using the Monte Carlo method for randomly selected burned grid cells (~20% grid cells in each region) across North America. The ranges of the various parameters were assigned according to previous studies (Table 5). Within the parameter ranges, we assigned normally distributed values for combustion completeness of live biomass and dead organic

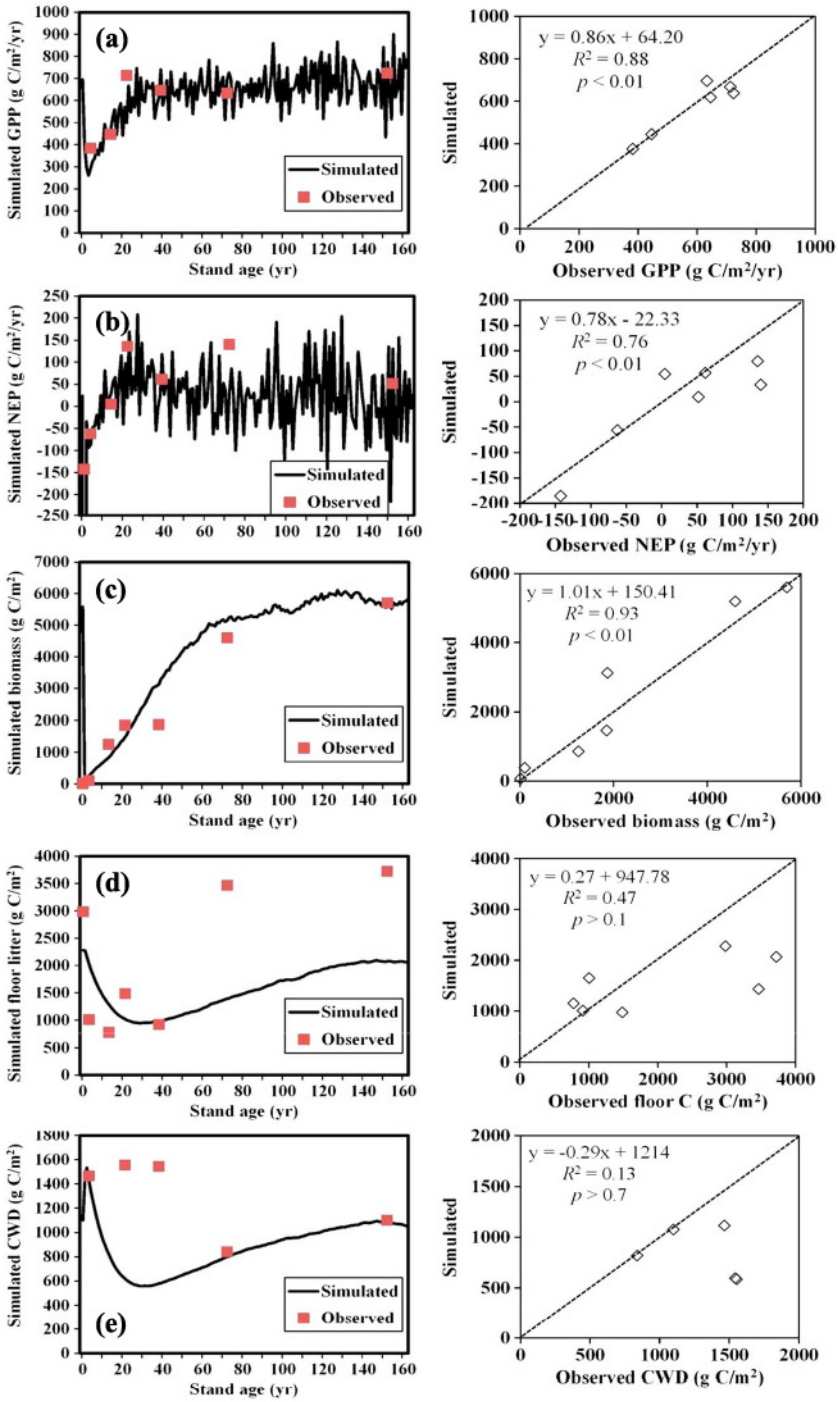

Figure 4. Comparisons between modeled and observed carbon variables for spruce forests along a fire chronosequence gradient. (a) GPP, (b) net ecosystem production (NEP, positive values denote carbon sink), (c) total living biomass, (d) forest floor litter carbon, and (e) coarse woody debris (CWD). Note that the right column figures are fitted 1:1 lines and the regression equations; the site information and observed data were described and obtained from *Goulden et al.* [2011] and *Bond-Lamberty et al.* [2004].

matters and vegetation mortality. Due to a large work load, we only selected 500 parameter sets (random combination of the selected four parameters in Table 5) to conduct model simulations for the uncertainty ranges of direct carbon emission and net ecosystem carbon balance. We calculated the coefficient of variation (CV; 1 SD/mean) based on the selected 20% grid cells and propagated the CV to the entire North America study area.

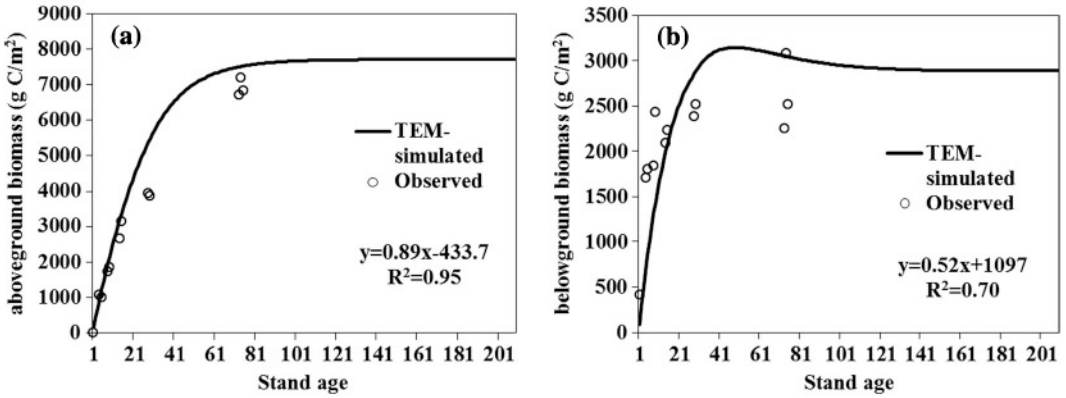

Figure 5. Comparisons between modeled and observed (a) aboveground and (b) belowground biomass for a seasonal dry tropical forest along a fire chronosequence gradient in Mexico (data source: Vargas *et al.* [2008]).

3. Results

3.1. Burn Area and Spatiotemporal Pattern in North America

The integrated burn area data indicated that the mean annual burn area was 3246 km^2, 17,627 km^2, 16,331 km^2, and 11,068 km^2 for Alaska (1940–2012), Canada (1920–2012), CONUS (1984–2012), and Mexico (1996–2012), respectively (Figure 7). The annual burn area accounted for about 0.25%, 0.21%, 0.22%, and 0.59% of the total land area in the four regions, respectively. Burn area had a large interannual variation with no significant change trends for Alaska, Canada, and Mexico, but a significant linear increasing trend (931 km^2/yr; $p < 0.05$) from 1984 to 2012 in CONUS. For Alaska and Canada, burn area during 1990–2012 (5552 and 20,202 km^2/yr, respectively; $p < 0.05$) was significantly higher than the corresponding long-term

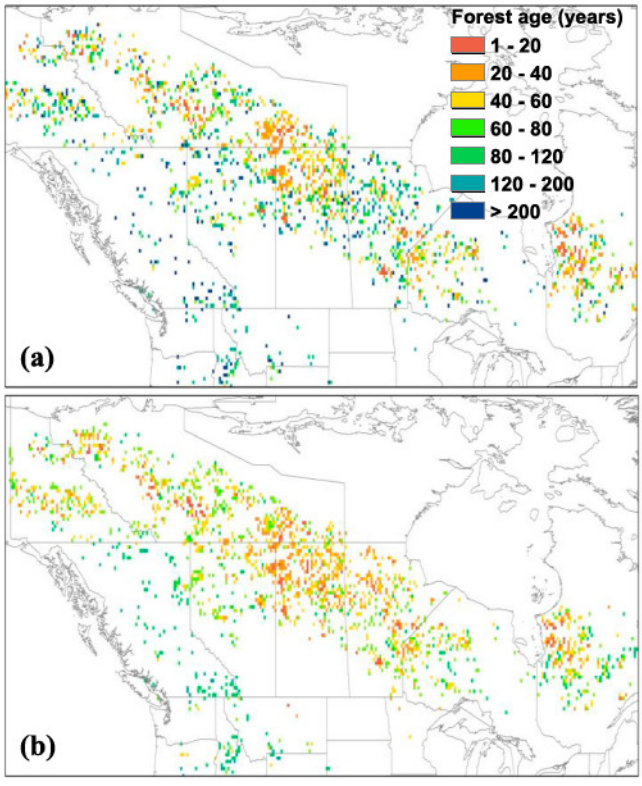

Figure 6. (a and b) Comparisons of forest age structure induced by wildland fires (this study) with inventory forest age data [source: *Pan et al.*, 2012] in Canada.

Table 5. Uncertainty Ranges (±1 SD) for Various Parameters Influencing Ecosystem Carbon Dynamic

Variables	Ranges	References	Uncertainty Ranges (±1 SD)	
			Direct Carbon Emission	NECB
Stem consumption completeness	50%	*Kurz et al.* [2008b]; *van der Werf et al.* [2010]	±17%	
Litter and deadwood consumption completeness	Alaska: 25%; Canada: 20%; CONUS and Mexico: 50%	*de Groot et al.* [2009]; *Kasischke and Hoy* [2012]; *van der Werf et al.* [2010]	±9.5%	
Duff consumption depth	50%	*Turetsky et al.* [2011]; *van der Werf et al.* [2010]	±16%	
Vegetation mortality	25%	*van der Werf et al.* [2010]	±10%	
Overall			±15%	±20%

average for each (3246 and 17,626 km^2/yr). For each region, the highest burn area years occurred in 2004, 1989, 2011, and 1998 in Alaska (27,783 km^2), Canada (70,921 km^2), CONUS (48,132 km^2), and Mexico (23,215 km^2), respectively. In Alaska, about 87% of fire events occurred in forests and taiga woodlands; about 64% and 48% of burn areas were in forest types for Canada and Mexico, respectively. In contrast, over 72% of the burn areas in CONUS occurred in herbaceous plants and shrubland. In Alaska, the highest mean annual burn area was scattered in the grid cells of central Alaska, with distributions of mostly black spruce forests and taiga woodlands (Figure 8a). In Canada, the highest burn area was displayed over the peatland area in Saskatchewan and Northwest Territories in Canada. In CONUS, the highest burn area was located in the western and central areas characterized by dry climate and mostly herbaceous or shrub plants, especially in California where the mean fire return interval was often less than 50 years. In Mexico, the highest burn area was distributed along the dry climate zone with primarily temperate or tropical dry forests. As compared to the mean annual burn area during the entire study period (1940–2012 for Alaska and 1920–2012 for Canada), we found a higher burn area during 1990–2012 in Alaska and less burned area in Canada.

3.2. Direct Carbon Emissions From Fire

Mean annual emissions varied significantly among years and were highly correlated with the mean annual burn area, with significant ($p < 0.01$) correlation coefficients (R^2) of 0.98, 0.96, 0.92, and 0.78 for Alaska, Canada, CONUS, and Mexico, respectively. Average direct carbon emissions (i.e., the combusted total carbon during fire events) in Alaska were 10.65 ± 4.02 Tg C/yr (1 Tg = 10^{12} g; ±2 SE) and 18.23 ± 2.74 Tg C/yr over 1940–2012 and 1990–2012, respectively (Table 6), with considerable interannual variability. Year 2004 was the year of peak emission in Alaska during the 2000s decade. The average carbon emission per unit burn area was 3.38 kg C/m^2/yr. The estimated average carbon emission was 47.77 ± 7.40 Tg C/yr (2.67 kg C/m^2/yr per

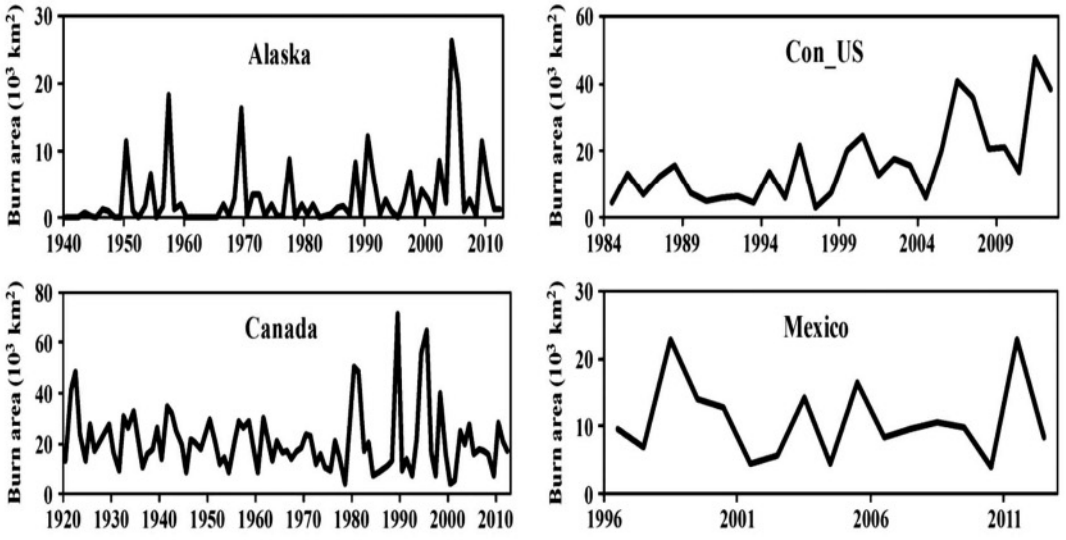

Figure 7. Interannual variation in burn area during the study periods (1940–2012 for Alaska, 1920–2012 for Canada, 1984–2012 for CONUS, and 1996–2012 for Mexico) in North America.

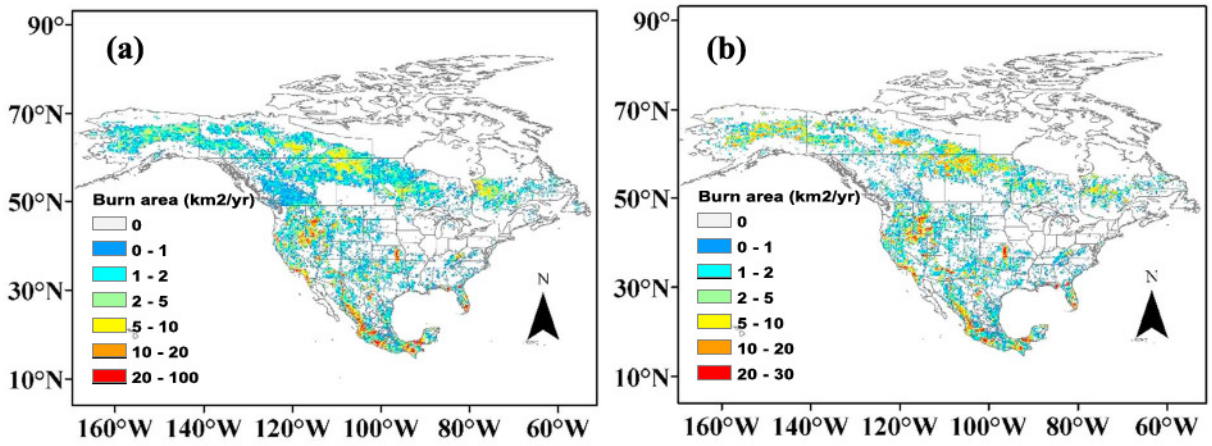

Figure 8. (a and b) Mean annual burned area for each 0.25° grid cell in North America during the entire observational periods (km^2/yr; Alaska: 1940–2012, Canada: 1920–2012, CONUS: 1984–2012, Mexico: 1996–2012) and 1990–2012 (km^2/yr). Note that the FRI-based burn area during 1990–1995 is used for Mexico to calculate the mean burn area during 1990–2012.

unit burn area) and 57.87 ± 8.68 Tg C/yr (2.87 g C/m^2/yr) in Canada during 1920–2012 and 1990–2012, respectively, with the peak emissions in 1989 and 1995. The average carbon emission was 17.05 ± 4.16 Tg C/yr (0.95 kg C/m^2/yr per unit burn area) and 13.40 ± 3.72 Tg C/yr (1.19 kg C/m^2/yr per unit of burn area) in CONUS and Mexico, respectively 1990–2012. The highest carbon emissions occurred in 2011 for both regions. During the common time period (1990–2012), the fire-induced direct carbon emissions for the entire North America were 107.86 ± 16.18, 105.55 ± 15.83, and 106.55 ± 13.33 Tg C/yr during 1990s, 2000s (i.e., 2000–2012), and 1990–2012, respectively.

In Alaska and Canada, the highest direct carbon emissions came from the combustion of the top layer SOM (duff), while the consumption of FFL was the largest cause of direct carbon emissions in CONUS and Mexico (Table 7). The mean burned SOM was 1.22 kg C/m^2/yr in the boreal regions of North America during 1990–2012, with an average reduction in duff layer depth of 7.5 ± 2 cm (Mean ± 2 SE). In Canada, the higher burn area and large proportion of forest as compared to other regions resulted in the consumption of large amounts of living biomass and CWD. The drier climate (i.e., higher DC_m values) and higher accumulation in the fine litter and duff layers resulted in greater direct carbon emissions per unit area in Alaska and Canada as compared with CONUS and Mexico. For the entire North America, the estimated mean annual combustions for living biomass, SDW, FFL, CWD, and SOM were 26.87, 0.20, 34.83, 13.26, and 31.40 Tg C/yr, respectively, during 1990–2012.

Table 6. Decadal Variations in Fire-Caused Direct Carbon Emissions (Tg C/yr; 1 Tg = 10^{12} g) From Terrestrial Ecosystems in North America

Time Periods	Alaska	Canada	CONUS	Mexico
1920–1929	–	50.62	–	–
1930–1939	–	41.71	–	–
1940–1949	1.29	38.78	–	–
1950–1959	14.33	44.87	–	–
1960–1969	7.53	38.08	–	–
1970–1979	6.79	36.56	–	–
1980–1989	5.67	74.78	11.53	–
1990–1999	12.88	71.00	8.10	15.88
2000–2012	22.35	47.77	23.93	11.49
Average1[a]	10.62	49.30	15.57	12.63
Average2[a]	18.23	57.87	17.05	13.40

[a]The average 2 is calculated for the period of 1990–2012, while average 1 is calculated based on the observational time periods for different regions (Alaska: 1940–2012; Canada: 1920–2012; CONUS: the conterminous U.S., 1984–2012; Mexico: 1996–2012).

Table 7. Fire-Affected Area and Direct Carbon Emissions (Tg C/yr) From Different Fuel Components in North America During 1990–2012[a]

Regions	Burn Area (km^2/yr)	Live Biomass	SDW	FFL	CWD	Duff
Alaska	5,552	2.45	0.00	5.92	1.71	8.45
Canada	20,202	12.47	0.03	15.77	6.36	23.25
CONUS	17,924	6.62	0.05	7.75	2.63	0.0
Mexico	11,273	5.33	0.12	5.39	2.56	0.0
NA	54,951	26.87	0.20	34.83	13.26	31.40

[a]CONUS: the conterminous US; NA: North America; SDW: standing dead wood; CWD: coarse woody debris; FFL: aboveground fine litter.

3.3. Changes in Net Ecosystem Carbon Balance

The effect of fire only (experiment 3; environmental factors keep constant) resulted in carbon sources in all regions of North America during 1990–2012 (Table 8). The changing environmental factors (experiment 2; no fire events) resulted in a large carbon sink in Alaska and Canada, but a large carbon source in CONUS and Mexico. Across North America, the environmental changes and fire disturbance (experiment 1) caused a large carbon sink during the 1990s and a carbon source during the 2000s. The interannual variation in NECB was primarily determined by environmental factors; however, its magnitude was greatly influenced by fire disturbance (experiment 3). The changing environmental factors resulted in a carbon sink of 13.85 ± 2.77 Tg C/yr, but fire disturbance (experiment 3) caused a higher carbon source of 40.10 ± 8.02 Tg C/yr in North America. There were large interactive effects between environmental factors and fire (experiment 1 − experiment 2 − experiment 3), resulting in reduced carbon emission in Alaska (2.02 Tg C/yr), Canada (9.82 Tg C/yr), CONUS (1.42 Tg C/yr), and Mexico (0.75 Tg C/yr) during 1990–2012 (Table 8). NPP in Canada and Alaska showed an increasing trend due to environmental change, which accelerated vegetation recovery after fire. In addition, the increasing trend in precipitation reduced the consumptions completeness of fuel (especially for the top layer SOM) in these regions. These explained the large negative interactions between environmental factors and fire. Overall, the fire-caused NECB (with interaction) was −26.09 ± 5.22 Tg C/yr for the entire North America during 1990–2012, with a mean carbon source of −34.95 and −19.27 Tg C/yr during the 1990s and 2000s, respectively. Fire combustion resulted in a larger direct carbon emission (106.55 Tg C/yr) during this period; however, the vegetation recovery offsets most of these emissions (by 80.46 Tg C/yr) through faster vegetation regrowth and slower dead organic matter accumulation.

As compared to the background fire history (i.e., the FRI-based fire history data), the changing fire regime (experiment1 − experiment4) caused a carbon source in Alaska, Canada, and CONUS due to larger burn area generated by the FRI approach during 1990–2012, indicating an increasing trend in fire effects on carbon emissions in these regions, especially for Alaska. The changing fire regime resulted in a small carbon sink in Mexico due to smaller burn area based on the FRI approach, implying a recovery trend in ecosystem

Table 8. Net Ecosystem Carbon Balance (Tg C/yr) Under the Influences of Multiple Environmental Factors and Fire in Alaska, Canada, Conterminous U.S. (CONUS), Mexico, and Entire North America During 1990–2012[a]

NECB	Alaska	Canada	CONUS	Mexico	NA (1990s)	NA (2000s)	NA (All)
ALL_FIRE (experiment 1)	22.60	139.03	−98.05	−49.73	141.42	−84.28	13.85
ALL_NOFIRE (experiment 2)	33.52	150.90	−94.51	−49.97	176.38	−65.01	39.94
FIRE_ONLY (experiment 3)	−12.94	−21.69	−4.96	−0.50	−47.69	−34.25	-40.10
ALL_FRI (experiment 4)	29.40	140.02	−95.16	−50.76	157.97	−79.93	23.51
Changing fire regime	−6.80	−0.99	−2.89	1.03	−16.55	−4.35	−9.65
Fire + interaction	−10.92	−11.87	−3.54	0.25	−34.95	−19.27	−26.09
Environment + interaction	35.54	160.72	−93.09	−49.22	189.11	−50.02	53.95
Fire legacy effects	18.86	71.06	15.29	10.16	116.43	117.84	117.22

[a]Effects of changing fire regime (experiment 1 − experiment 4); fire + interaction: effects of fire and interaction with environmental factors (experiment 1 – experiment 2); environment + interaction: effects of changing environmental factors and interaction with fire (experiment 1 − experiment 3); fire legacy effects: the legacy effects from prior fires (experiment 6 − experiment 2). The considered environmental factors include climate, atmospheric CO_2, land use and land cover, and tropospheric ozone. NA: entire North America.

Table 9. Changes in Carbon Stocks (g C/m^2/yr) of Different Fuel Components for Burned Areas in Different Regions of North America During 1990–2012[a]

1990–2012	Alaska	Canada	CONUS	Mexico
SOC	−1396.34	−980.04	−34.59	−7.53
VEGC	−474.64	446.15	−197.46	229.01
SDW	124.31	−18.44	49.84	−42.92
CWD	−8.95	−42.03	−2.91	−30.27
LITC	−213.40	6.24	−12.23	−35.24

[a]Negative values denote carbon release to atmosphere from this carbon pool. SDW: standing dead wood, CWD: coarse woody debris, VEGC: vegetation carbon, SOC: soil organic carbon, LITC: total litter C (including aboveground and belowground litter).

carbon stocks from previous fire disturbance. Overall, the changing fire regime caused a carbon source of 9.65 ± 1.93 Tg C/yr during 1990–2012 for the entire North America continent.

3.4. Changes in Carbon Stocks of Different Fuel Components

Due to difference in fire history, fuel loads, vegetation types, burn severity, and consumption completeness, the carbon stocks in different fuel components showed varying patterns during 1990–2012 (Table 9). In Alaska, the top layer SOM was the major carbon source and followed by vegetation carbon pool, while SDW was a net carbon sink. In Canada, SOM was the major source of fire-caused carbon emissions. SDW and CWD were small sources, while vegetation biomass was a large net carbon sink due to faster vegetation recovery under the influences of environmental changes and smaller burn area during 1990–2012. The consumption of SOM from the duff layer, drier climate (higher DC_m), and slower recovery resulted in large carbon emissions from the soil organic carbon pool in both Alaska and Canada. In CONUS, the vegetation carbon pool was the largest carbon source, followed by SOC, LITC, and SDW, while STD was the only carbon sink. The annual burn area in CONUS showed an increasing trend since the 1980s, resulting in a reduction for most carbon pools (Figure 7). In Mexico, the vegetation carbon pool was a large carbon sink due to smaller burn area as compared to background fire history (i.e., FRI-based fire history) and the legacy effects of fire events before 1990, while other carbon pools were a net carbon source. It is notable that the belowground litter (i.e., dead roots) generally increased after fire events due to no direct fire consumption of the dead roots, which slightly offset the total carbon loss from aboveground litter carbon and SOM.

Due to legacy effects of higher fire severity, more fuel loads of dead organic matters, and direct consumption of top layer SOM, the variations in SOC, vegetation carbon (VEGC), and LITC were larger in Canada and Alaska as compared to those in CONUS and Mexico (Figure 9). The highest fire-caused net carbon emissions (< -50 g C/m^2/yr) from living vegetation were primarily shown in the boreal forest regions, such as interior Alaska and the Canadian managed forest area (Figure 9a); this is mainly due to the more frequent fire events and slower biomass recovery rate in these areas during 1990–2012. The largest increase (>30 g C/m^2/yr) in living biomass was found in the Canadian managed forest area due to the legacy effects from historical fire events, as well as smaller burn area and reduced fire frequency during recent decades. In CONUS and Mexico, due to less intensive and frequent burning in forest area and smaller burn proportion (Figure 8), the grid-cell level averaged changes in vegetation carbon pool was small than that in Alaska and Canada. The largest decreases in SOC were found in the peatland area (with high SOC content and low recovery rate) and the relatively drier boreal regions (e.g., the interior Alaska, Manitoba, and Saskatchewan; Figure 9b). This was primarily caused by the direct consumption of top layer soil organic matter. On the other hand, the collective effects of high litter stocks and high DC_m values (Figure 3) caused large amount of aboveground dead organic matter to be consumed by fire, resulting in less aboveground dead organic matter inputs to the soil. The consumption of large amount of dead organic matter by fire caused reductions in carbon stocks of the dead organic matter pool in Canada and Alaska (Figure 9c); however, the increasing inputs of unconsumed aboveground biomass and belowground dead roots after fire greatly offset the carbon losses from direct fire consumption and resulted in carbon sinks for most of the burned area in North America during 1990–2012.

Combining the carbon fluxes from all pools, the highest net fire-caused carbon sources (< -50 g C/m^2/yr) were generally located in the grid cells with the highest mean annual burn area in Canada and Alaska (Figures 8 and 9d). The frequent burning in forests and interactions with environmental changes resulted

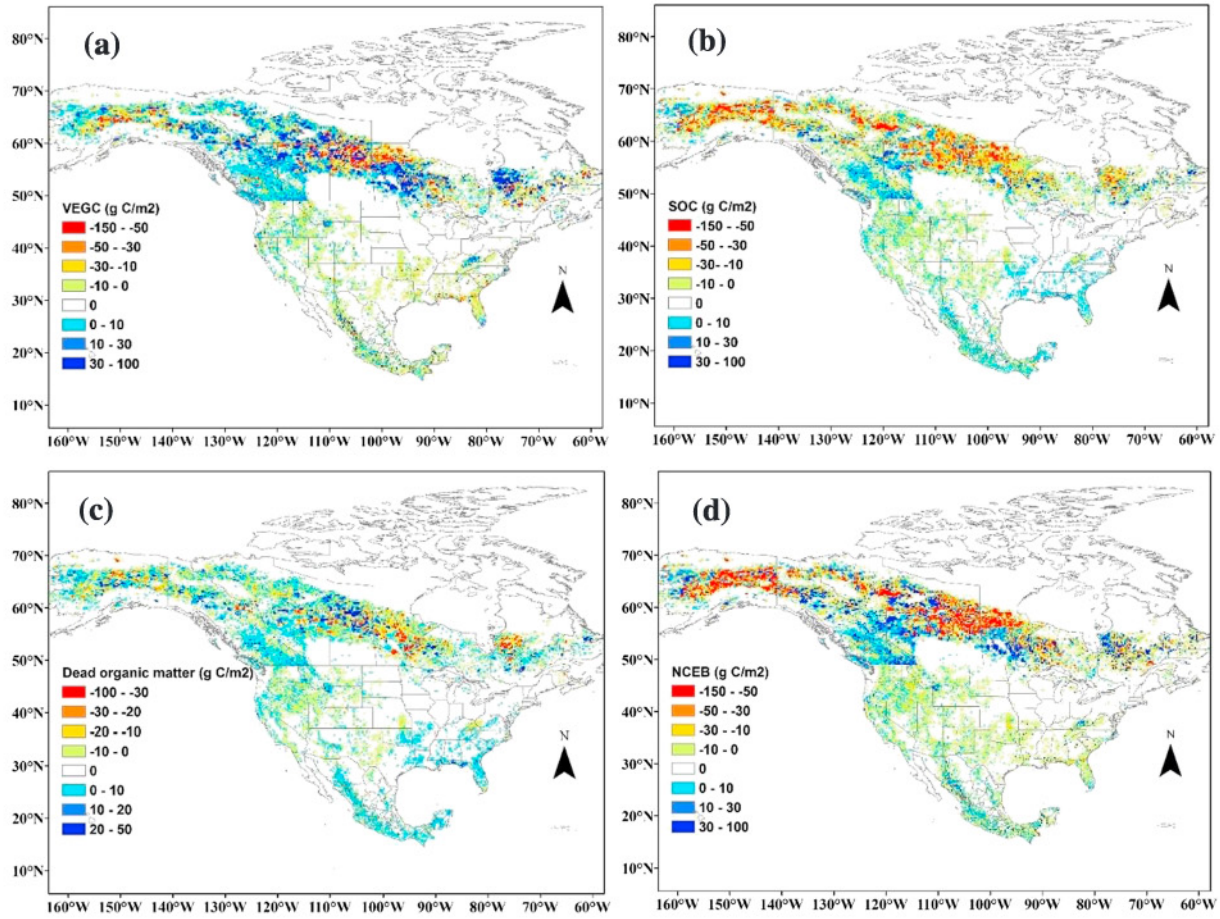

Figure 9. Spatial distribution in fire-caused net carbon fluxes from (a) live biomass (g C/m^2/yr), (b) soil organic carbon (g C/m^2/yr), (c) dead organic matter (g C/m^2/yr; including aboveground and belowground litter, CWD, and SDW), and (d) net ecosystem carbon balance (NECB; including carbon fluxes from all carbon pools; g C/m^2/yr) at 0.25° resolution in North America during 1990–2012. Note that negative values denote carbon release from the land ecosystem to atmosphere.

in large direct carbon emissions and slow recovery in the live biomass and dead organic matter pools in these regions. There were also some areas with moderate annual burn area but had the highest carbon emissions in Alaska and Canada, primarily located in the peatland area with dry climate and large amount of floor litter carbon and top-layer SOM (duff). In Canada, carbon sinks were primarily found in the southwest area due to legacy effects and reduced burn area, which was illustrated in the comparison between the different spatial patterns in Figures 8a and 8b. In CONUS and Mexico, the highest burn area was generally located in the regions dominated by shrubland or grassland, resulting in smaller carbon sources or sinks as compared those in Alaska and Canada. In addition, due to less intensive and frequent burning in forest area and smaller burn forest fractions in a grid cell, the grid-cell level changes in NECB were small over these two regions.

4. Discussion

4.1. Comparisons Against Other Studies in North America

During the past two decades, many studies have been conducted to estimate fire disturbance effects on direct carbon emissions and net ecosystem carbon balance at site and regional scales across North America. Both the interannual variation patterns and magnitudes of direct carbon emissions from this study were generally consistent ($R^2 > 0.88; p < 0.01$) with reports from *Amiro et al.* [2001] over Canada (Figure 10a) and *Giglio et al.* [2013] (GFED4) over boreal North America (Canada and Alaska) (Figure 10b), with slightly higher estimates in TEM primarily during the peak emission years. Our estimates were higher than GFED4 for CONUS (Figure 10c), and both studies displayed an increasing trend during 1997–2012. In Mexico, our estimate was generally lower than that from GFED4, especially in 1998, but the interannual variation

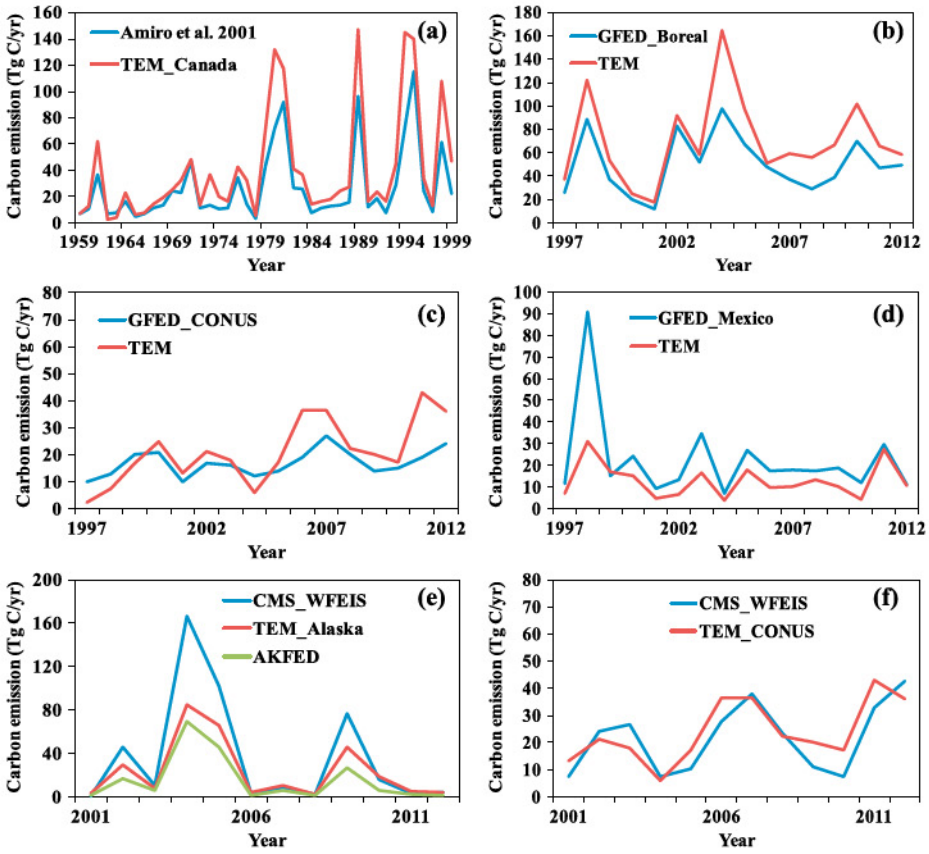

Figure 10. Comparisons between TEM-simulated fire-caused direct carbon emissions with other previous studies at different regions. (a) Canada, (b) boreal: boreal North America including Canada and Alaska, (c) CONUS, (d) Mexico, (e) Alaska, and (f) CONUS. Note that AKFED data were from *Veraverbeke et al.* [2015] and CMS-WFEIS data were from *French et al.* [2016].

pattern between both estimates was quite similar (Figure 10d). In Alaska, our results tended to underestimate direct carbon emissions in the years with peak emissions as compared to the NASA Carbon Monitoring System (CMS) annual wildland fire emissions (CMS_WFEIS v0.5) [*French et al.*, 2016]; however, our estimations were consistently higher than the estimate from Alaskan Fire Emissions Database (AKFED) [*Veraverbeke et al.*, 2015], especially in the peak emission years (Figure 10e). The interannual variations were similar as compared to these two previous estimations. In CONUS, both the magnitudes and interannual variations of our estimates were consistent with that from CMS_WFEIS (Figure 10f). The estimated fire-caused carbon fluxes in this study were also compared to estimates from other studies as shown in Table 10. Our estimates of fuel consumption and associated direct carbon emissions were generally higher than other studies in Canada and Alaska, but at the same time generally lower than other estimates in CONUS. In Mexico, *Vicente et al.* [2014] estimated that fire-caused carbon emissions were 418.57 g C/m^2/yr over burn areas (3.03 Tg C/yr), which is substantially lower than our estimate (1230 g C/m^2/yr; 13.40 Tg C/yr; Figure 10d) and GFED4 (22.32 Tg C/yr). Our estimated NECB was slightly lower than that reported by *Hayes et al.* [2011] for Alaska and Canada during 1997–2006 but was substantially lower than that of *Balshi et al.* [2007, 2009] for the 1980–2010 period. Using the previous version of TEM, *Balshi et al.* [2007] estimated a higher direct carbon emission than our study. In addition, our study used the longest available burn area data to represent the historical fire legacy effects before 1990, while the updated version of TEM (v6.1) better represents vegetation recovery trajectories and dead organic matter dynamics. These mechanisms together result in the slower recovery of carbon in vegetation and dead organic matter pools in our simulations, as shown in Figures 4 and 5.

4.2. The Role of Fire Disturbance in Determining Ecosystem Carbon Balance

Fire disturbance is generally recognized as a major cause of carbon transfer from land to atmosphere at regional scales due to the large amount of direct carbon emissions during combustion [*Balshi et al.*, 2007;

Table 10. The Comparisons of Direct Carbon Emission and Net Ecosystem Carbon Balance Between This Study and Other Previous Studies

Regions[a]	Variables	Time Period	This Study	Others	References
Canada	Direct carbon emission	1990–2008	58.51 Tg C/yr	23 ± 16 Tg C/yr[b]	*Stinson et al.* [2011]
Canada	Floor fuel consumption	1959–1999	1.48 kg C/m^2	2.44 kg C /m^2[c]	*Amiro et al.* [2001]
Canada	Floor fuel consumption	1960–2000	1.48 kg C/m^2	1.3 kg C/m^2	*Schultz et al.* [2008]
Canada	Direct carbon emission	1959–1999	54.42 Tg C/yr	27 Tg C/yr	*Amiro et al.* [2001]
Canada	Direct carbon emission	1959–1995	54.55 Tg C/yr	41 Tg C/yr	*Balshi et al.* [2007]
CONUS	Direct carbon emission	2002–2006	27.76 Tg C/yr	58.25 ± 13.64 Tg C/yr[d]	*Wiedinmyer and Neff* [2007]
CONUS	Direct carbon emission	1984–2005	14.43 Tg C/yr	19.32 Tg C/yr	*Goetz et al.* [2012]
CONUS	Direct carbon emission	2003–2012	25.22 Tg C/yr	35 Tg C/yr	*Kaiser et al.* [2012]
CONUS	Direct carbon emission	2002–2012	24.84 Tg C/yr	33.2 Tg C/yr	*Wiedinmyer et al.* [2011]
CONUS	Direct carbon emission	1984–2010	13.81 Tg C/yr	16.1 Tg C/yr	*Yang et al.* [2015a]
CONUS	Direct carbon emission	1995–2011	19.06 Tg C/yr	23.5 Tg C/yr	*Zhang et al.* [2014]
Alaska	Floor fuel consumption	1960–2000	2.79 kg C/m^2	1.9 kg C/m^2	*Schultz et al.* [2008]
Alaska	Floor fuel consumption	2006–2008	2.94 kg C/m^2	1.5–3.0 kg C/m^2	*Kasischke and Hoy* [2012]
Alaska	Direct carbon emission	2002–2006	38.15 Tg C/yr	21.82 ± 24.27 Tg C/yr[e]	*Wiedinmyer and Neff* [2007]
Alaska and Canada	Direct carbon emission	1971–1991	62.60 Tg C/yr	42 Tg C/yr	*Conard and Ivanova* [1997]
Alaska and Canada	Direct carbon emission	1980–1994	79.22 Tg C/yr	53 Tg C/yr	*French et al.* [2004]
Alaska	Fire-caused NECB	1980–1989	−1.23 Tg C/yr	−5 to −12 Tg C/yr	*Balshi et al.* [2007]
Canada and Alaska	Fire-caused NECB	1997–2006	−16.12 Tg C/yr	−23.1 Tg C/yr[f]	*Hayes et al.* [2011]
Canada and Alaska	Fire-caused NECB	1991–2000	−26.86 Tg C/yr	~ −45 Tg C/yr	*Balshi et al.* [2009]
Canada and Alaska	Fire-caused NECB	2000–2010	−12.87 Tg C/yr	~ −50 Tg C/yr	*Balshi et al.* [2009]
Mexico	Direct carbon emission	1999–2010	13.40 Tg C/yr	3.03 Tg C/yr	*Vicente et al.* [2014]

[a]For NECB, negative values denote carbon releases from land ecosystems to atmosphere, while for direct carbon emission, positive values denote carbon source.
[b]Only from managed forest (forest fires account for 45% of all fire area).
[c]2.0 is used to convert carbon to biomass.
[d]This estimate was actually the maximum emission rate as inferred from their estimation methods.
[e]Soil duff burning was not considered.
[f]A small part of Canada was not included in *Hayes et al.*'s study.

Bond-Lamberty et al., 2007; *Hayes et al.*, 2011]. In addition, long-term legacy effects are caused by microenvironmental changes, removal of the soil organic layer in burning, vegetation recovery, and carbon emissions from decomposition after fire. Previous studies suggested that fire disturbance could result in permanent thawing of permafrost soil in the boreal region and thus cause large carbon release in the long term [e.g., *Yuan et al.*, 2012; *Genet et al.*, 2013]. However, fires also can alter ecosystem vegetation composition, structure, soil nutrient, and water conditions, as well as microenvironment, which could alter postfire carbon uptake and therefore determine the long-term balance between fire emissions and postfire carbon uptake. The ultimate role of fire in the regional or continental-scale carbon balance depends on the complex interactions among fire properties, climate, atmospheric CO_2, nutrient availability, and other ecosystem properties. Whether fire disturbance results in a carbon sink or source over short-to-long-term time periods depends on the fire severity and frequency; therefore, the effect of stand age has been considered to be an important factor in explaining the contemporary carbon sink in North America [*Kurz and Apps*, 1999; *Liu et al.*, 2011; *Kasischke et al.*, 2013].

Our study indicated that fire disturbance resulted in a direct carbon emission of 106.55 ± 15.98 Tg C/yr during 1990–2012 in North America, which accounts for about 22.57% of the terrestrial carbon sink on the continent (472 Tg C/yr; median value among multiple estimation approaches [*King et al.*, 2015]), implying that fire is an important agent disrupting the overall terrestrial carbon dynamics. *Hayes et al.* [2012] estimated that Canada was an overall net carbon sink of 124.6 Tg C/yr (median value estimated by forward models from *Hayes et al.* [2012]) during 2000–2006. Our study estimates that fire-caused direct carbon emissions were 57.87 Tg C/yr in Canada during this period, corroborating the finding by *Bond-Lamberty et al.* [2007] that fire disturbance was a major driver of carbon dynamics at the national scale. Similarly, fire disturbance played a more important role in ecosystem carbon dynamics in Mexico. The fire-caused carbon emission estimate is 10.57 ± 4.44 Tg C/yr during 2000–2006, while the overall environmental changes resulted in a carbon source of 8.70 Tg C/yr (median value estimated by inverse models from *Hayes et al.* [2012]) in Mexico. For the entire U.S. (including Alaska and CONUS), the fire-caused carbon emission is 48.84 ± 16.15 Tg C/yr during 2000–2006, accounting for about 13.68% of the net carbon sink (357 Tg C/yr; median number estimated

by forward models from *Hayes et al.* [2012]), induced by multiple environmental changes. As predicted by *Balshi et al.* [2009], annual burn area at the end of 21st century will be 3–4 times higher than current values in the boreal region. Together with increasing atmospheric CO_2 levels and climate-driven drought intensity, the importance of fire-caused direct emissions for continental-scale terrestrial carbon dynamics is likely to be intensified in the near future.

Fire-driven carbon dynamics in terrestrial ecosystems include three components: (1) the legacy effects from historical fires, (2) the present direct carbon emission and ecosystem recovery, and (3) the interactions between fire and other environmental factors. Historical legacies of fire disturbance shape current ecosystem function and affect long-term trajectories of ecological change [*Foster et al.*, 2003]. Therefore, to accurately track net ecosystem carbon balance caused by fire disturbance for a specific period, models need to simulate all three components [*Gough et al.*, 2007]. In this study, we estimated that the legacy effects from historical fires before 1990 were 117.22 Tg C/yr (including the interaction between historical fires and environmental factors; Table 7) for North America, which served as a large and continuous carbon sink during 1990–2012. When combining the direct carbon emissions, the ecosystem recovery, with the legacy effects from historical fires, the net ecosystem carbon source was 26.09 ± 5.22 Tg C/yr during 1990–2012, which accounts for only about 5.53% of the mean annual terrestrial carbon uptake rate, indicating a small impact on the overall, long-term net terrestrial ecosystem carbon balance in North America. *Yang et al.* [2015b] estimated a significantly higher fire-caused carbon source (140 Tg C/yr) during 1900–2010 as compared to our study and several previous estimates (Table 9), which was primarily due to the lack of consideration of the large fire legacy effects, which assumed no fire occurrence before 1900. This implies the importance of fire legacy effects and using the long-term fire records in simulating ecosystem carbon dynamics. In our study, we collected the long-term (especially for Alaska and Canada) fire records to estimate NECB in 1990–2012, which may provide a more robust estimation, particularly with respect to legacy effects.

We found that the interannual variation in net ecosystem carbon balance across North America was primarily determined (the determination coefficient is close to1.00) by the environmental factors considered in this study (i.e., climate, atmospheric CO_2, and ozone), while the magnitude was determined by the effects of fire disturbance. *Bond-Lamberty et al.* [2007] also found that the magnitude of the net ecosystem carbon balance in Canadian boreal forests was driven by changes in fire disturbance from 1948 to 2005, while climate change determined the interannual variability. The negative interactions between environmental changes and fire disturbance caused a reduction of fire-caused net carbon emission by 14.01 Tg C/yr across North America in the 2000s (calculated as fire + interaction minus fire only; experiment3, in Table 8), suggesting that it is important to include environmental changes when studying fire disturbance effects.

4.3. Sources of Fire-Caused Net Ecosystem Carbon Fluxes

Fire is reported to either directly or indirectly influence many terrestrial carbon pools, and its effects are variable and depend on fire severity, timing, frequency, geomorphological characteristics, environmental conditions, and ecosystem types [*Johnson and Curtis*, 2001; *Kasischke et al.*, 2011; *Turetsky et al.*, 2011]. The varied combinations of these factors can result in large spatial and temporal variability in postfire ecosystem carbon fluxes and ecosystem recovery trajectories. These factors and their interactions can cause a large uncertainty in estimating fire effects, and it is difficult to attain sufficiently accurate results with methodologies based on just a few factors or carbon pools. TEM has been widely used to simulate the fire effects on soil thermal dynamics [*Zhuang et al.*, 2003], soil biogeochemistry [*Zhuang et al.*, 2002], dead organic matter dynamics [*Genet et al.*, 2013], and NECB [*Zhuang et al.*, 2002; *Balshi et al.*, 2007, 2009; *Yuan et al.*, 2012; *Kelly et al.*, 2016] in North America, and its performance has been extensively evaluated against field and inventory data as well as other estimates. Although fire consumes portions of the living biomass and dead organic matter carbon pools, the increasing inputs of unconsumed standing dead wood, coarse woody debris, and belowground litter (i.e., dead roots) following a fire could offset some of the carbon loss from combustion and result in an overall net carbon sink. Particularly, in the boreal region, these increased carbon stocks in the dead organic carbon pools following fire will decompose very slowly under a cold and dry climate, as well as in nutrient-limited conditions. Many previous studies [e.g., *van der Werf et al.*, 2010; *Balshi et al.*, 2007; *Yuan et al.*, 2012] have not explicitly addressed the issue for fire-caused carbon gains in dead root biomass and their dynamics over a long-term period. Moreover, the accelerated nutrient release by direct fire consumption and indirect fire-caused microenvironment changes could lessen limitations for plant growth in

nutrient-limited environments, thus further resulting in a small carbon sink as compared to the prefire ecosystem [*Jiang et al.*, 2015], especially for short-lived vegetation (e.g., herbaceous plants and shrubs). These would greatly offset the net ecosystem carbon fluxes due to fire.

Stinson et al. [2011] estimated that about 4 Tg C/yr living biomass and 19 Tg C/yr of dead organic matter were burned in the managed forests in Canada during 1990–2008. Our study also indicated that the consumption of surface dead organic matter were the major contributors to the total fire-caused carbon source in Canada and Alaska. The highest burn area and most frequent fire events were found in the peatland distribution area [*Turetsky et al.*, 2015]. The carbon accumulations in forest floor litter and top-layer SOM (duff) in this region could be more than 10 kg C/m^2 [*de Groot et al.*, 2009; *Kasischke and Hoy*, 2012; *Turetsky et al.*, 2011]. Under the interactions of high fire severity and dry climate, the surface dead organic matter may be mostly consumed by fire and thus contribute to high carbon emissions in this region [*Turetsky et al.*, 2011, 2015]. Due to cold climate and frequent fire disturbances, the recovery of forest floor organic matter in boreal regions could take a longer time than in other regions. Through sensitivity analysis, we found that the soil organic matter took over a hundred years to recover to prefire conditions after one fire event for a spruce forest in a peatland area in Canada, although vegetation biomass can be restored within a shorter time period (around 60 years). In addition, frequent fire events cause slow biomass recovery of shrublands and forest in dry climate regions such as in the western CONUS and arid temperate forests in Mexico, resulting in a large net carbon source from the biomass pool.

4.4. Uncertainties and Limitations

The direct emissions of carbon from fires and the ecosystem carbon dynamics after fire are both highly uncertain due to the combined errors and uncertainties in the model framework and model driving data. Uncertainties in the fire emission estimates may arise from the burn area data, the identification of burned vegetation types and locations, the assumptions made in the fuel loading, the amount and completeness of burned fuel, and the assigned emission factors. Based on the approaches described in studies by *French et al.* [2004, 2011] and *van der Werf et al.* [2010], we assessed the uncertainties resulting from combustion completeness and vegetation mortality for selected about using the Monte Carlo method. The resulting uncertainty (1 SD) for direct carbon emission is ±15% of the mean values and ±20% of the mean values for net ecosystem carbon balance. Uncertainties in the other model parameters and input data may greatly amplify our estimated uncertainty ranges.

The limitations of TEM in simulating fire-caused carbon dynamics have been described in *Balshi et al.* [2009]. In this study, we have reduced some model uncertainties through improved model mechanisms and parameterization methods; however, there are still many limitations. First, there is still substantial uncertainty associated with the parameters that affect fire emissions and the fate of carbon after fire in our model. Finally, future studies should conduct a more comprehensive assessment of error associated with these parameters. Second, due to the lack of a longer historical burn area data record, we are unable to track the long-term legacy effects of fire before our study periods. The FRI-based tracking of historical fires may not be accurate and could compound the fire legacy effects, especially for CONUS and Mexico, where only short-term historical fire data records are available. Third, the tracking of postfire vegetation succession is also an important aspect to represent in models for accurately assessing postfire ecosystem carbon dynamics. Generally, forest fire disturbance creates a series of successional stages such as grassland, shrubland, and then forest [*Johnson*, 1992]. However, we did not consider vegetation succession after fire disturbance in this study, as the vegetation type of each cohort was the same before and after fire disturbance. This may either overestimate or underestimate carbon uptake at the early succession stage of forests depending on factors such as fire severity and postdisturbance environmental conditions. Finally, our study did not consider the effects of fire on permafrost thaw, which could drive a long-term legacy effects on soil organic matter decomposition in the boreal permafrost region [*Kasischke and Hoy*, 2012; *Turetsky et al.*, 2011; *Yuan et al.*, 2012]. Thus, our study may also underestimate fire-caused carbon releases in the boreal region of North America.

5. Conclusions

The occurrence of extremely large and severe fire events in Alaska, Canada, and CONUS during recent years has drawn much attention to the fire contributions to terrestrial carbon dynamics in North America. No

consensus about fire contribution to carbon budget in North America has been reached thus far [*Hayes et al.*, 2012; *Kasischke et al.*, 2011; *King et al.*, 2015]. This lack of consensus is primarily due to the difficulty in isolating the fire-caused net ecosystem carbon flux, especially assessing the legacy effects from historical fire events. With the improvement in model parameterization and the application of long-term observational burn area data and associated fire characteristics, our study attempted to simulate the fire-caused direct carbon emission and net ecosystem carbon balance of North America during 1990–2012. The improvements in estimation methods and data in this study may greatly reduce the model uncertainty and provide a more reliable and systematic assessment for fire effects on carbon dynamics. Based on the field observational data and existing regional estimates from the previous publications, we evaluated the TEM model performance in simulating carbon dynamics after fires. The simulation results showed good consistency between the simulated and observed carbon fluxes and pools. Our study estimates fire-caused direct carbon emissions of 106.55 ± 15.98 Tg C/yr during 1990–2012, while net ecosystem carbon balance associated with fire was a much smaller source of 26.09 ± 5.22 Tg C/yr. This highlights a substantial carbon resequestration after fire across North American land ecosystems due to the historical fire legacy effects, the changing fire regime, and interactions with changing environmental factors. The fire-caused net ecosystem carbon fluxes were small as compared to the best estimates of carbon uptake, implying that fire disturbance may not have substantially altered the net terrestrial ecosystem carbon balance in North America during recent decades.

Acknowledgments

This study is supported by the DOE Early Career Award through DOE-BER program (award: 3ERKP818), the U.S. Geological Survey Alaska Climate Science Center's Cooperative Agreement (G10AC00588 and 11AC20291), and the National Science Foundation through the Bonanza Creek LTER (award: 1026415). We thank the two anonymous reviewers and Brendan M. Rogers for providing insightful and valuable comments and suggestions, which significantly help improve this paper. Any use of trade, firm, or product names is for descriptive purposes only and does not imply endorsement by the U.S. Government. The original data are available from the corresponding author upon request through e-mail (auburncgs@gmail.com).

References

Amiro, B. D., J. B. Todd, B. M. Wotton, K. A. Logan, M. D. Flannigan, B. J. Stocks, J. A. Mason, D. L. Martell, and K. G. Hirsch (2001), Direct carbon emissions from Canadian forest fires, 1959 to 1999, *Can. J. For. Res.*, *31*, 512–525.

Amthor, J. S., et al. (2001), Boreal forest CO_2 exchange and evapotranspiration predicted by nine ecosystem process models: Intermodel comparisons and relationships to field measurements, *J. Geophys. Res.*, *106*, 33,623–33,648.

Balshi, M. S., et al. (2007), The role of historical fire disturbance in the carbon dynamics of the pan-boreal region: A process-based analysis, *J. Geophys. Res.*, *112*, G02029, doi:10.1029/2006JG000380.

Balshi, M. S., A. D. McGuire, P. Duffy, M. Flannigan, D. W. Kicklighter, and J. Melillo (2009), Vulnerability of carbon storage in North American boreal forests to wildfires during the 21st century, *Global Change Biol.*, *15*, 1491–1510.

Barrett, S., D. Havlina, J. Jones, W. Hann, C. Frame, D. Hamilton, K. Schon, T. Demeo, L. Hutter, and J. Menakis (2010), Interagency Fire Regime Condition Class Guidebook. Version 3.0, Homepage of the Interagency Fire Regime Condition Class website, USDA Forest Service, US Department of the Interior, and the Nature Conservancy, p. 126. [Available at https://www.frames.gov/partner-sites/frcc/frcc-home/.]

Bond-Lamberty, B., S. D. Peckham, D. E. Ahl, and S. T. Gower (2007), Fire as the dominant driver of central Canadian boreal forest carbon balance, *Nature*, *450*, 89–92.

Bond-Lamberty, B., C. Wang, and S. T. Gower (2004), Net primary production and net ecosystem production of a boreal black spruce wildfire chronosequence, *Global Change Biol.*, *10*, 473–487.

Bousquet, P., et al. (2006), Contribution of anthropogenic and natural sources to atmospheric methane variability, *Nature*, *443*, 439–443.

Brandt, J. P. (2009), The extent of the North American boreal zone, *Environ. Rev.*, *17*, 101–161.

Chapin, F. S., II, et al. (2006), Reconciling carbon-cycle concepts, terminology, and methods, *Ecosystems*, *9*, 1041–1050.

Conard, S. G., and G. A. Ivanova (1997), Wildfire in Russian boreal forests—Potential impacts of fire regime characteristics on emissions and global carbon balance estimates, *Environ. Pollut.*, *98*, 305–313.

de Groot, W. J., J. M. Pritchard, and T. J. Lynham (2009), Forest floor fuel consumption and carbon emissions in Canadian boreal forest fires, *Can. J. For. Res.*, *39*, 367–382.

Euskirchen, E. S., A. D. McGuire, F. S. Chapin III, S. Yi, and C. C. Thompson (2009), Changes in vegetation in northen Alaska under scenarios of climate change, 2003–2100: Implications for climate feedbacks, *Ecol. Appl.*, *19*, 1022–1043.

Felzer, B. S., J. Reilly, J. Melillo, D. W. Kicklighter, M. Sarofim, C. Wang, R. G. Prinn, and Q. Zhuang (2005), Future effects of ozone on carbon sequestration and climate change policy using a global biochemistry model, *Clim. Change*, *73*, 345–373.

Felzer, B. S., T. W. Cronin, J. M. Melillo, D. W. Kicklighter, and C. A. Schlosser (2009), Importance of carbon-nitrogen interactions and ozone on ecosystem hydrology during the 21st century, *J. Geophys. Res.*, *114*, G01020, doi:10.1029/2008JG000826.

Flannigan, M. D., and C. E. van Wagner (1991), Climate change and wildfire in Canada, *Can. J. For. Res.*, *21*, 66–72.

Foster, D., F. Swanson, J. Aber, I. Burke, N. Brokaw, D. Tilman, and A. Knapp (2003), The importance of land-use legacies to ecology and conservation, *Bioscience*, *53*, 77–88.

French, N. H. F., et al. (2011), Model comparisons for estimating carbon emissions from North American wildland fire, *J. Geophys. Res.*, *116*, G00K05, doi:10.1029/2010JG001469.

French, N. H. F., P. Goovaerts, and E. S. Kasischke (2004), Uncertainty in estimating carbon emissions from boreal forest fires, *J. Geophys. Res.*, *109*, D14S08, doi:10.1029/2003JD003635.

French, N. H. F., et al. (2016), *Annual Wildland Fire Emissions (WFEIS v0.5) for Conterminous US and Alaska, 2001–2013*, ORNL DAAC, Oak Ridge, Tenn., doi:10.3334/ORNLDAAC/1306.

Genet, H., et al. (2013), Modeling the effects of fire severity and climate warming on active layer thickness and soil carbon storage of black spruce forests across the landscape in interior Alaska, *Environ. Res. Lett.*, *8*(4), 045016, doi:10.1088/1748-9326/8/4/045016.

Giglio, L., G. R. van der Werf, J. T. Randerson, G. J. Collatz, and P. S. Kasibhatla (2013), Global estimation of burned area using MODIS active fire observations, *Atmos. Chem. Phys.*, *6*, 957–974.

Girardin, M. P., and B. M. Wotton (2009), Summer moisture and wildfire risks across Canada, *J. Appl. Meteorol. Climatol.*, *48*, 517–533.

Goetz, S. J., et al. (2012), Observations and assessment of forest carbon dynamics following disturbance in North America, *J. Geophys. Res.*, *117*, G02022, doi:10.1029/2011JG001733.

Gough, C. M., C. S. Vogel, K. H. Harrold, K. George, and P. S. Curtis (2007), The legacy of harvest and fire on ecosystem carbon storage in a north temperate forest, *Global Change Ecol.*, *13*, 1935–1949.
Goulden, M., A. McMillan, G. Winston, A. Rocha, K. Manies, J. Harden, and B. Bond-Lamberty (2011), Patterns of NPP, GPP, respiration, and NEP during boreal forest succession, *Global Change Biol.*, *17*, 855–871.
Harden, J. W., S. E. Trumbore, B. J. Stocks, A. Hirsch, S. T. Gower, K. P. O'Neill, and E. S. Kasischke (2000), The role of fire in the boreal carbon budget, *Global Change Biol.*, *6*, 174–184.
Hayes, D. J., A. D. McGuire, D. W. Kicklighter, K. R. Gurney, T. J. Burnside, and J. M. Melillo (2011), Is the northern high-latitude land-based CO_2 sink weakening?, *Global Biogeochem. Cycles*, *25*, GB3018, doi:10.1029/2010GB003813.
Hayes, D. J., et al. (2012), Reconciling estimates of the contemporary North American carbon balance among terrestrial biosphere models, atmospheric inversions, and a new approach for estimating net ecosystem exchange from inventory-based data, *Global Change Biol.*, *18*, 1282–1299.
Hurteau, M. D., and M. L. Brooks (2011), Short- and long-term effects of fire on carbon in US dry temperate forest systems, *Bioscience*, *6*, 139–146.
Hurtt, G. C., S. W. Pacala, P. R. Moorcroft, J. Caspersen, E. Shevliakova, R. A. Houghton, and B. Moore III (2002), Projecting the future of the U.S. carbon sink, *Proc. Natl. Acad. Sci. U.S.A.*, *99*, 1389–1394.
Ito, A., and J. E. Penner (2004), Global estimates of biomass burning emissions based on satellite imagery for the year 2000, *J. Geophys. Res.*, *109*, D14S05, doi:10.1029/2003JD004423.
Jiang, Y., E. B. Rastetter, A. V. Rocha, A. R. Pearce, B. L. Kwiatkowski, and G. Shaver (2015), Modeling carbon-nutrient interactions during the early recovery of tundra after fire, *Ecol. Appl.*, *25*(6), 1640–1652.
Johnson, D. W., and P. S. Curtis (2001), Effects of forest management on soil C and N storage: Meta analysis, *For. Ecol. Manage.*, *140*, 227–238.
Johnson, E. A. (1992), *Fire and Vegetation Dynamics: Studies from the North American Boreal Forest*, pp. 1–129, Cambridge Univ. Press, Cambridge, New York.
Kaiser, J., A. Heil, M. Andreae, A. Benedetti, N. Chubarova, L. Jones, J. J. Morcrette, M. Razinger, M. Schultz, and M. Suttie (2012), Biomass burning emissions estimated with a global fire assimilation system based on observed fire radiative power, *Biogeosciences*, *9*(1), 527–554.
Kashian, D. M., W. H. Romme, D. B. Tinker, M. G. Turner, and M. G. Ryan (2006), Carbon storage on landscapes with stand-replacing fires, *Bioscience*, *56*, 598–606.
Kasischke, E. S., and E. E. Hoy (2012), Controls on carbon consumption during Alaskan wildland fires, *Global Change Biol.*, *18*, 685–699.
Kasischke, E. S., and M. R. Turetsky (2006), Recent changes in the fire regime across the North American boreal region—Spatial and temporal patterns of burning across Canada and Alaska, *Geophys. Res. Lett.*, *33*, L09703, doi:10.1029/2006GL025677.
Kasischke, E. S., T. Loboda, L. Giglio, N. H. F. French, E. E. Hoy, B. de Jong, and D. Riano (2011), Quantifying burned area for North American forests: Implications for direct reduction of carbon stocks, *J. Geophys. Res.*, *116*, G04003, doi:10.1029/2011JG001707.
Kasischke, E. S., D. Williams, and D. Barry (2002), Analysis of the patterns of large fires in the boreal forest region of Alaska, *Int. J. Wildland Fire*, *11*, 131–144.
Kasischke, E. S., B. D. Amiro, N. N. Barger, N. H. F. French, S. J. Goetz, G. Grosse, M. E. Harmon, J. A. Hicke, S. Liu, and J. G. Masek (2013), Impacts of disturbance on the terrestrial carbon budget of North America, *J. Geophys. Res. Biogeosci.*, *118*, 303–316, doi:10.1002/jgrg.20027.
Kelly, R., H. Genet, A. D. McGuire, and F. S. Hu (2016), Paleodata-informed modeling of large carbon losses from recent burning of boreal forests, *Nat. Clim. Change*, *6*, 79–82.
King, A. W., D. J. Hayes, D. N. Huntzinger, T. O. West, and W. M. Post (2012), North America carbon dioxide sources and sinks: Magnitude, attribution, and uncertainty, *Front. Ecol. Environ.*, *10*, 512–519.
King, A. W., et al. (2015), North America's net terrestrial carbon exchange with the atmosphere 1990–2009, *Biogeosciences*, *12*, 399–414.
Kurz, W. A., and M. J. Apps (1999), A 70-year retrospective analysis of carbon fluxes in the Canadian forest sector, *Ecol. Appl.*, *9*, 526–547.
Kurz, W. A., et al. (2009), CBM-CFS3: A model of carbon-dynamics in forestry and land-use change implementing IPCC standards, *Ecol. Modell.*, *220*, 480–504.
Kurz, W. A., G. Stinson, and G. Rampley (2008a), Could increased boreal forest ecosystem productivity offset carbon losses from increased disturbances?, *Philos. Trans. R. Soc. B*, *363*, 2259–2268.
Kurz, W. A., G. Stinson, G. J. Rampley, C. C. Dymond, and E. T. Neilson (2008b), Risk of natural disturbances makes future contribution of Canada's forests to the global carbon cycle highly uncertain, *Proc. Natl. Acad. Sci. U.S.A.*, *105*, 1551–1555.
Liu, S., et al. (2011), Simulating the impacts of disturbances on forest carbon cycling in North America: Processes, data, models, and challenges, *J. Geophys. Res.*, *116*, G00K08, doi:10.1029/2010JG001585.
Loveland, T. R., B. C. Reed, J. F. Brown, D. O. Ohlen, J. Zhu, L. Yang, and J. W. Merchant (2000), Development of a global land cover characteristics database and IGBP DISCover from 1-km AVHRR data, *Int. J. Remote Sens.*, *21*, 1303–1330.
Lu, X., D. W. Kicklighter, J. M. Melillo, J. M. Reilly, and L. Xu (2015), Land carbon sequestration within the conterminous United States: Regional- and state-level analyses, *J. Geophys. Res. Biogeosci.*, *120*, 379–398, doi:10.1002/2014JG002818.
McGuire, A. D., J. S. Clein, J. M. Melillo, D. W. Kicklighter, R. A. Meier, C. J. Vorosmarty, and M. C. Serreze (2000a), Modeling carbon responses of tundra ecosystems to historical and projected climate: Sensitivity of pan-arctic carbon storage to temporal and spatial variation in climate, *Global Change Biol.*, *6*, 141–159.
McGuire, A. D., J. M. Melillo, J. T. Randerson, W. J. Parton, M. Heimann, R. A. Meier, J. S. Clein, D. W. Kicklighter, and W. Sauf (2000b), Modeling the effects of snowpack on heterotrophic respiration across northern temperate and high latitude regions: Comparison with measurements of atmospheric carbon dioxide in high latitudes, *Biogeochemistry*, *48*, 91–114.
Meigs, G. W., D. C. Donato, J. L. Campbell, J. G. Martin, and B. E. Law (2009), Forest fire impacts on carbon uptake, storage, and emission: The role of burn severity in the eastern Cascades, Oregon, *Ecosystems*, *12*, 1246–1267.
Pan, Y., J. M. Chen, R. Birdsey, K. McCullough, L. He, and F. Deng (2012), NACP Forest age maps at 1-km resolution for Canada (2004) and the U.S.A. (2006). Data set. Available on-line [http://daac.ornl.gov] from ORNL DAAC, Oak Ridge, Tenn.
Ramankutty, N., and J. A. Foley (1999), Estimating historical changes in global land cover: Croplands from 1700 to 1992, *Global Biogeochem. Cycles*, *13*, 997–1027.
Rogers, B. M., A. J. Soja, M. L. Goulden, and J. T. Randerson (2015), Influence of tree species on continental differences in boreal fires and climate feedbacks, *Nat. Geosci.*, *8*(3), 228–234.
Schmoldt, D. L., D. L. Peterson, R. E. Keane, J. M. Lenihan, D. McKenzie, D. R. Weise, and D. V. Sandberg (1999), *Assessing the Effects of Fire Disturbance on Ecosystems: A Scientific Agenda for Research and Management*, *Gen. Tech. Rep. PNW-GTR-455*, pp. 1–104, USDA Forest Service, Pacific Northwest Research Station, Portland, Oreg.
Schultz, M. G., A. Heil, J. J. Hoelzemann, A. Spessa, K. Thonicke, J. G. Goldammer, A. C. Held, J. Pereira, and M. van Het Bolscher (2008), Global wildland fire emissions from 1960 to 2000, *Global Biogeochem. Cycle*, *22*(2), GB2002, doi:10.1029/2007GB003031.

Stinson, G., et al. (2011), An inventory-based analysis of Canada's managed forest carbon dynamics, 1990 to 2008, *Global Change Biol.*, *17*, 2227–2244.

Stocks, B. J., and J. B. Kauffman (1997), Biomass consumption and behavior of woodland fires in boreal, temperate, and tropical ecosystems: Parameters necessary to interpret historic fire regimes and future fire scenarios, in *Sediment Records of Biomass Burning and Global Change*, *NATO ASI Series 51*, edited by J. S. Clark et al., pp. 169–188, Springer, Berlin.

Turetsky, M. R., E. S. Kane, J. W. Harden, R. D. Ottmar, K. L. Manies, E. Hoy, and E. S. Kasischke (2011), Recent acceleration of biomass burning and carbon losses in Alaskan forests and peatlands, *Nat. Geosci.*, *4*, 27–31.

Turetsky, M. R., B. Benscoter, S. Page, G. Rein, G. R. van der Werf, and A. Watts (2015), Global vulnerability of peatlands to fire and carbon loss, *Nat. Geosci.*, *8*, 11–14.

van der Werf, G. R., J. T. Randerson, G.vJ. Collatz, L. Giglio, P. S. Kasibhatla, A. F. Arellano, S. C. Olsen, and E. S. Kasischke (2004), Continental-scale partitioning of fire emissions during the 1997 to 2001 El Nino/La Nina period, *Science*, *303*(5654), 73–76.

van der Werf, G. R., J. T. Randerson, L. Giglio, G. J. Collatz, M. Mu, P. S. Kasibhatla, D. C. Morton, R. S. DeFries, Y. Jin, and T. T. van Leeuwen (2010), Global fire emissions and the contribution of deforestation, savanna, forest, agricultural, and peat fires (1997–2009), *Atmos. Chem. Phys.*, *10*, 11,707–11,735.

Vargas, R., M. F. Allen, and E. B. Allen (2008), Biomass and carbon accumulation in a fire chronosequence of a seasonally dry tropical forest, *Global Change Biol.*, *14*, 109–124.

Veraverbeke, S., B. M. Rogers, and J. T. Randerson (2015), CARVE: Alaskan Fire Emissions Database (AKFED), 2001–2013, ORNL DAAC, Oak Ridge, Tenn., doi:10.3334/ORNLDAAC/1282.

Vicente, F. B., N. Carbajal, and L. F. P. Martínez (2014), Estimation of total yearly CO_2 emissions by wildfires in Mexico during the period 1999–2010, *Adv. Meteorol.*, *2014*, 8, doi:10.1155/2014/958457.

Wei, Y., et al. (2014), The North American carbon program multi-scale synthesis and terrestrial model intercomparison project: Part 2. Environmental driver data, *Geosci. Model Dev.*, *7*, 2875–2893.

Wiedinmyer, C., and J. C. Neff (2007), Estimates of CO_2 from fires in the United States: Implications for carbon management, *Carbon Balance Manage.*, *2*, doi:10.1186/1750-0680-2-10.

Wiedinmyer, C., S. K. Akagi, R. J. Yokelson, L. K. Emmons, J. A. Al-Saadi, J. J. Orlando, and A. J. Soja (2011), The Fire Inventory from NCAR (FINN): A high resolution global model to estimate the emissions from open burning, *Geosci. Model Dev.*, *4*(3), 625–641.

Yang, J., H. Tian, B. Tao, W. Ren, S. Pan, Y. Liu, and Y. Wang (2015a), A growing importance of large fires in conterminous United States during 1984–2012, *J. Geophys. Res. Biogeosci.*, *120*, 2625–2640, doi:10.1002/2015JG002965.

Yang, J., H. Tian, B. Tao, W. Ren, S. Pan, Y. Wang, and Y. Liu (2015b), Century-scale patterns and trends of global pyrogenic carbon emissions and fire influences on terrestrial carbon balance, *Global Biogeochem. Cycles*, *29*, 1549–1566, doi:10.1002/2015GB005160.

Yi, S., et al. (2009), Interactions between soil thermal and hydrological dynamics in the response of Alaska ecosystems to fire disturbance, *J. Geophys. Res.*, *114*, G02015, doi:10.1029/2008JG000841.

Yi, S., A. D. McGuire, E. Kasischke, J. Harden, K. Manies, M. Mack, and M. Turetsky (2010), A dynamic organic soil biogeochemical model for simulating the effects of wildfire on soil environmental conditions and carbon dynamics of black spruce forests, *J. Geophys. Res.*, *115*, G04015, doi:10.1029/2010JG001302.

Yuan, F., S. Yi, A. D. McGuire, K. D. Johnson, J. Liang, J. Harden, E. S. Kasischke, and W. Kurz (2012), Assessment of historical boreal forest C dynamics in Yukon River basin: Relative roles of warming and fire regime change, *Ecol. Appl.*, *22*, 2091–2109.

Yue, X., L. J. Mickley, J. A. Logan, and J. O. Kaplan (2013), Ensemble projections of wildfire activity and carbonaceous aerosol concentrations over the western United States in the mid-21st century, *Atmos. Environ.*, *77*, 767–780.

Zhang, X., S. Kondragunta, and D. P. Roy (2014), Interannual variation in biomass burning and fire seasonality derived from geostationary satellite data across the contiguous United States from 1995 to 2011, *J. Geophys. Res. Biogeosci.*, *119*, 1147–1162, doi:10.1002/2013JG002518.

Zhuang, Q., A. D. McGuire, J. Harden, K. P. O'Neill, V. E. Romanovsky, and J. Yarie (2002), Modeling soil thermal and carbon dynamics of a fire chronosequence in interior Alaska, *J. Geophys. Res.*, *107*, 8147, doi:10.1029/2001JD001244.

Zhuang, Q., A. D. McGuire, and J. M. Melillo (2003), Carbon cycling in extratropical terrestrial ecosystems of the northern hemisphere during the 20th century: A modeling analysis of the influences of soil thermal dynamics, *Tellus*, *55B*, 751–776.